Molecular Cell, Volume *77*

Supplemental Information

PIKES Analysis Reveals Response to Degraders and Key Regulatory Mechanisms of the CRL4 Network

Kurt M. Reichermeier, Ronny Straube, Justin M. Reitsma, Michael J. Sweredoski, Christopher M. Rose, Annie Moradian, Willem den Besten, Trent Hinkle, Erik Verschueren, Georg Petzold, Nicolas H. Thomä, Ingrid E. Wertz, Raymond J. Deshaies, and Donald S. Kirkpatrick

Figure S1 (related to Figure 1)

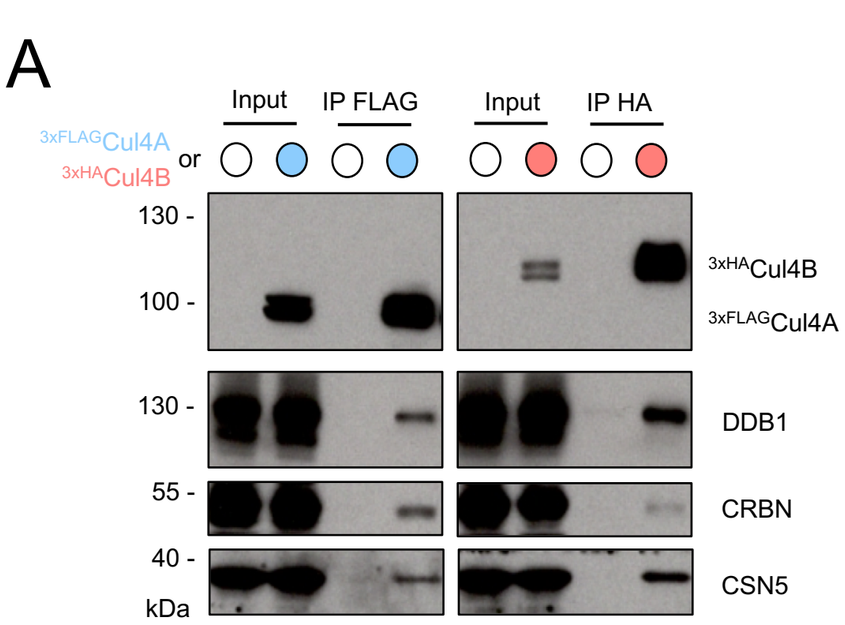

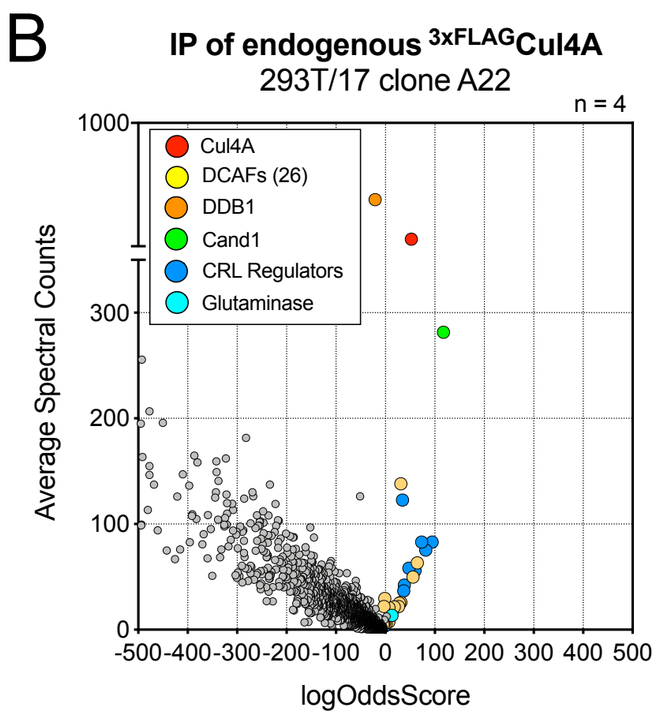

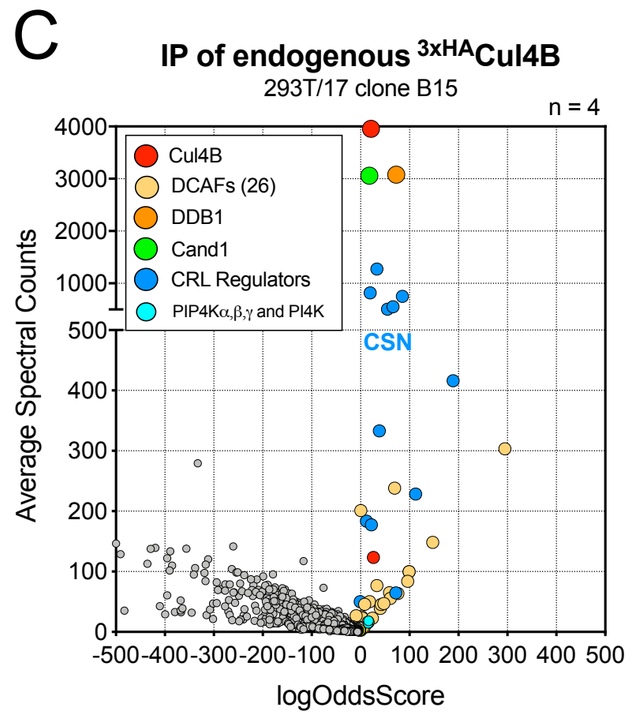

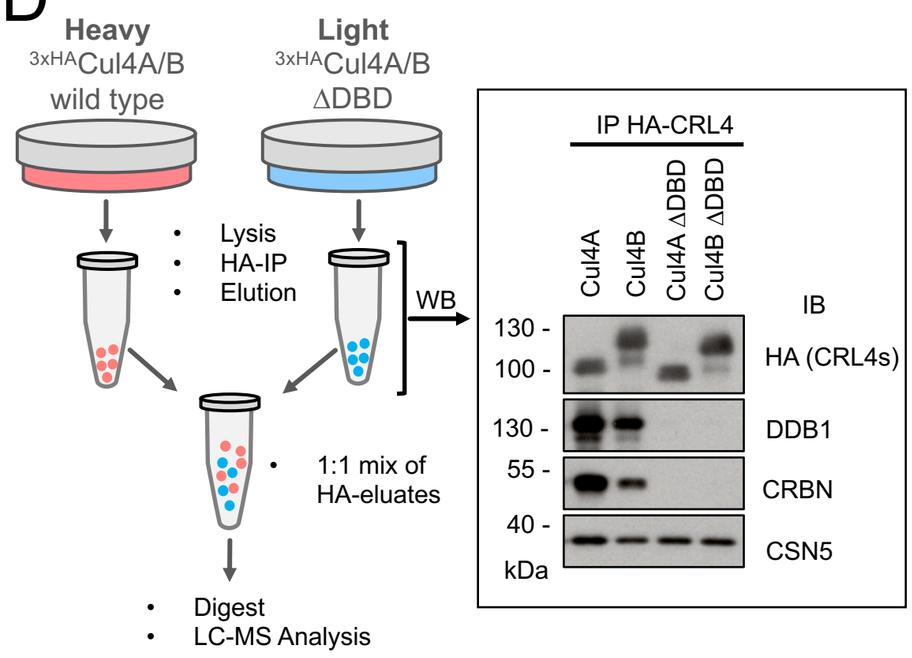

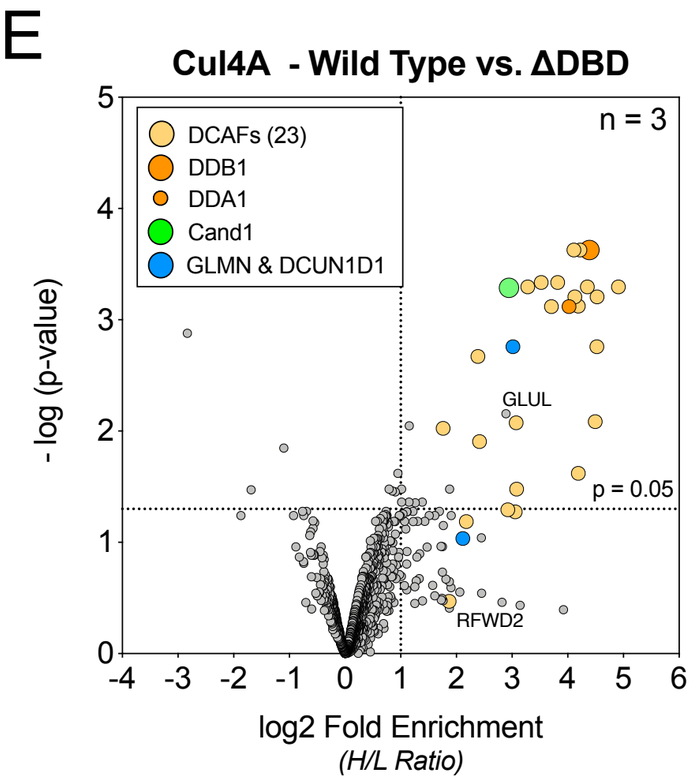

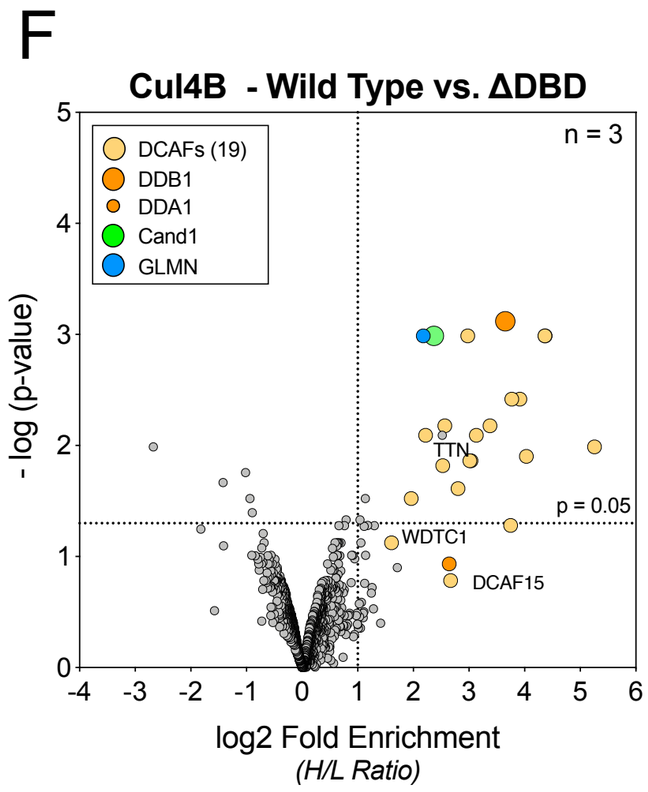

G

Composition of endogenous CRL4 Complexes

No	Gene	WD Domain	DBD# dependent	PSMs& in CUL4A IP	PSMs in CUL4B IP	Uniprot ID
	CUL4A			435	990#	Q13619
	CUL4B			20*	3955	Q13620
	RBX1		No	4*	123	P62877
	NEDD8		No	8	178	Q15843
	DDB1	Yes (21)	Yes	627	3079	Q16531
	DDA1	No	Yes	12*	23	Q9BW61
1	VPRBP	Yes (5)	Yes	138	304	Q9Y4B6
2	DDB2	Yes (7)	Yes	63	238	Q92466
3	AMBRA1	Yes (3)	Yes	30*	201	Q9C0C7
4	DCAF11	Yes (7)	Yes	50	148	Q8TEB1
5	BRWD3	Yes (9)	Yes	5*	100	Q6RI45
6	TRPC4AP	No	Yes	9	100	Q8TEL6
7	WDTC1	Yes (7)	Yes	22	84	Q8N5D0
8	DCAF6	Yes (7)	Yes	21	77	Q58WW2
9	CRBN	No	Yes	25	65	Q96SW2
10	BRWD1	Yes (8)	No	3*	64	Q9NSI6
11	DCAF8	Yes (7)	Yes	22	56	Q5TAQ9
12	DCAF10	Yes (7)	Yes	30*	50	Q5QP82
13	DTL	Yes (7)	Yes	26	47	Q9NZJ0
14	PHIP	Yes (8)	Yes	16*	46	Q8WWQ0
15	DCAF5	Yes (6)	Yes	7	45	Q96JK2
16	DCAF12	Yes (6)	Yes	8	39	Q5T6F0
17	PWP1	Yes (7)	Yes	15*	27*	Q13610
18	DCAF4	Yes (2)	Yes	7*	25	Q8WV16
19	ERCC8	Yes (7)	Yes	22	23	Q13216
20	DCAF16	No	Yes	6	17	Q9NXF7
21	TOR1AIP2	No	Yes	6	16	Q9H496
22	DCAF15	No	Yes	1*	8	Q66K64
23	DET1	No	Yes	ND	8	Q7L5Y6
24	RFWD2	Yes (7)	Yes	ND	7	Q8NHY2
25	DCAF17	No	Yes	ND	3*	Q5H9S7
26	DCAF4L1	Yes (2)	No	ND	3	Q3SXM0
	CAND1		Yes	282	3061	Q86VP6
	COPS1		No	75	505	Q13098
	COPS2		No	83	552	P61201
	COPS3		No	83	817	Q9UNS2
	COPS4		No	123	1272	Q9BT78
	COPS3		No	58	750	Q92905
	COPS6		No	56	416	Q7L5N1
	COPS7A		No	42	333	Q9UBW8
	COPS7B		No	21	229	Q9H9Q2
	COPS8		No	37	184	Q99627
	COPS9		No	1*	50*	Q8WXC6
	DCUN1D1		Yes	3*	6	Q96GG9
	GLMN		Yes	ND	65	Q92990
	UBXN7		ND	ND	2*	O94888

* BFDR > 0.05
# DBD = DDB1 Binding Domain on Cul4A/B
& PSM = Peptide spectral match
ND = Not detected

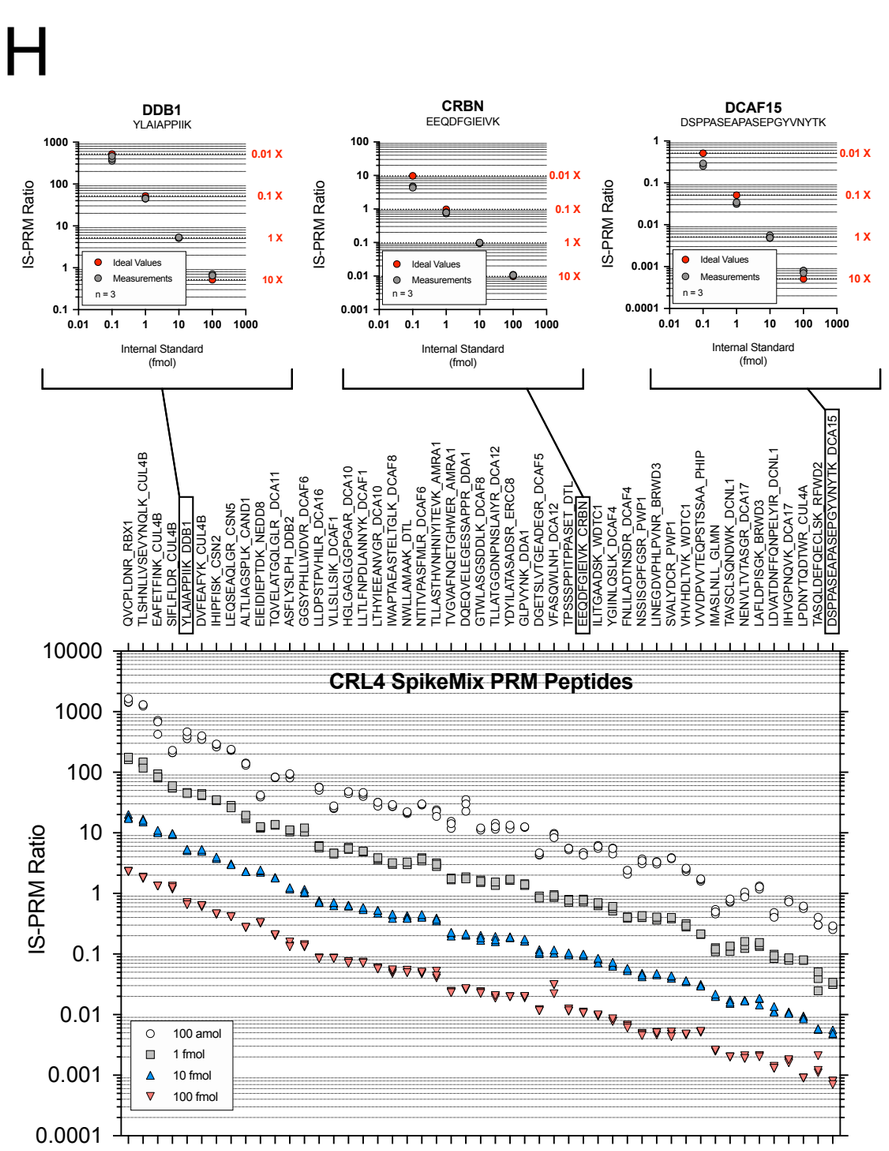

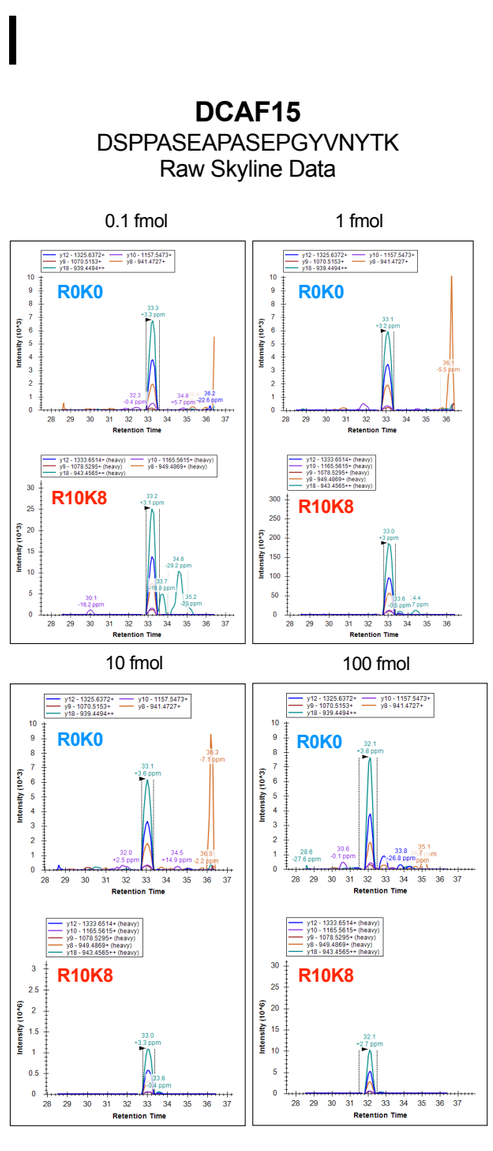

Figure Supplement 1. A toolbox to study endogenous CRL4 complexes, Related to Figure 1. (A-C) 293T/17$^{3xFLAG\text{-}Cul4A}$ (clone A22) and 293T/17$^{3xHA\text{-}Cul4B}$ (clone B15) were lysed and immunoprecipitated via anti-FLAG and anti-HA resin followed by elution of CRL4 complexes and LC-MS analysis. SDS-PAGE and western blot analysis (A) confirms successful capture of intact CRL4 complexes and specifically enriched proteins are pictured in (B-C) two volcano-plot like graphs featuring average spectral counts and logOddsScores. (D-F) 293T/17 cells were either grown in heavy (R6K8) SILAC medium or light medium and transiently transfected with wild type 3xHA-Cul4A or Cul4B (heavy labeled cells) or a 3xHA-Cul4A/B deletion mutant missing the DDB1-binding domain (ΔDBD) (light labeled cells). (D) Cells were lysed and immunoprecipitated via anti-HA resin followed by elution and 1:1 mixing of Cul4A/B wild type and Cul4A/BΔDBD complexes followed by LC-MS analysis. (E-F) Volcano plots showing DDB1-dependent Cul4 interacting proteins significantly enriched in the analyzed immunoprecipitates. (G) Table summarizing the composition of endogenous CRL4 complexes based on experiments displayed in (A-F). (H-F) Assessment of CRL4 SpikeMix PRM MS assay. Immunoprecipitated Cul4B complexes were eluted and digested followed by addition of CRL4 SpikeMix standards at four different concentrations and PRM analysis. (H) Displayed are the PRM ratios of all successfully targeted and detected peptides on a log scale as well as the ratio to concentration relationship for three peptides with a high (DDB1), medium (CRBN) and low PRM-Ratio (DCAF15). (I) Raw Skyline chromatograms of the lowest abundant peptide in the assay.

Figure S2 (related to Figure 2)

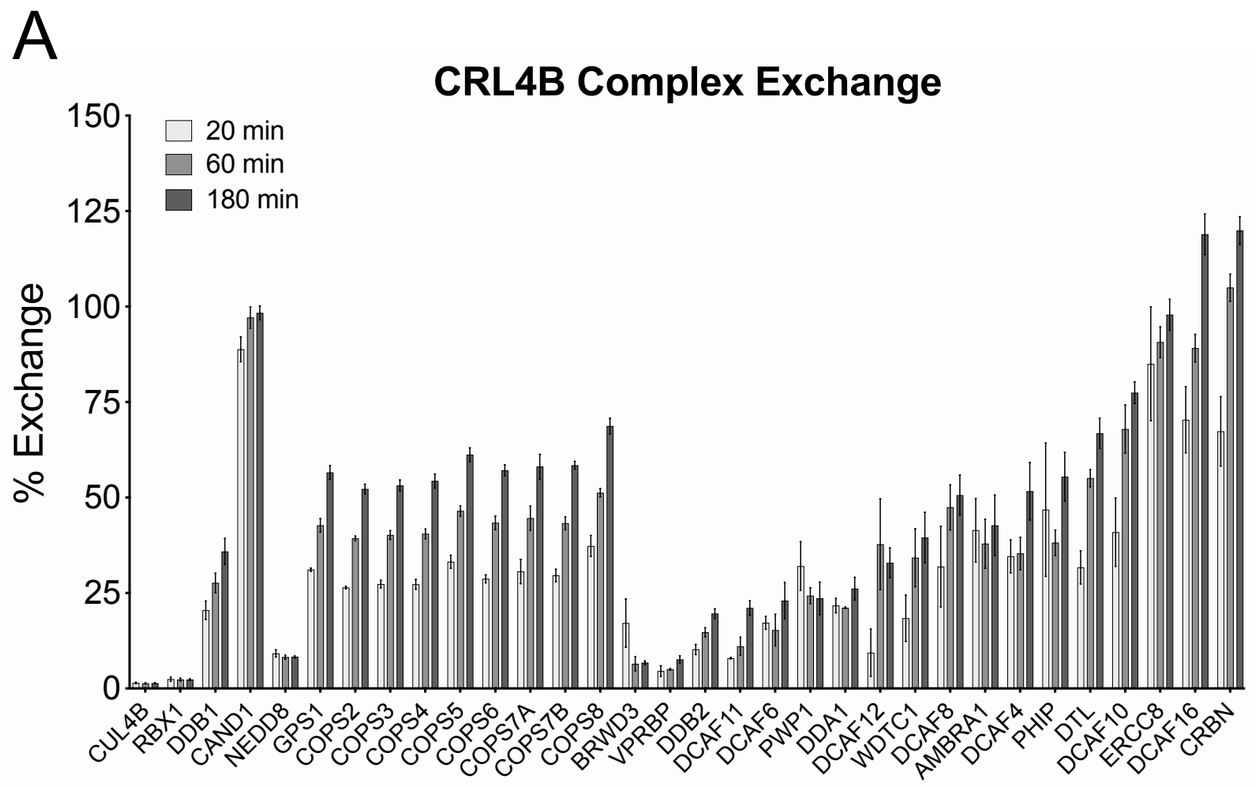

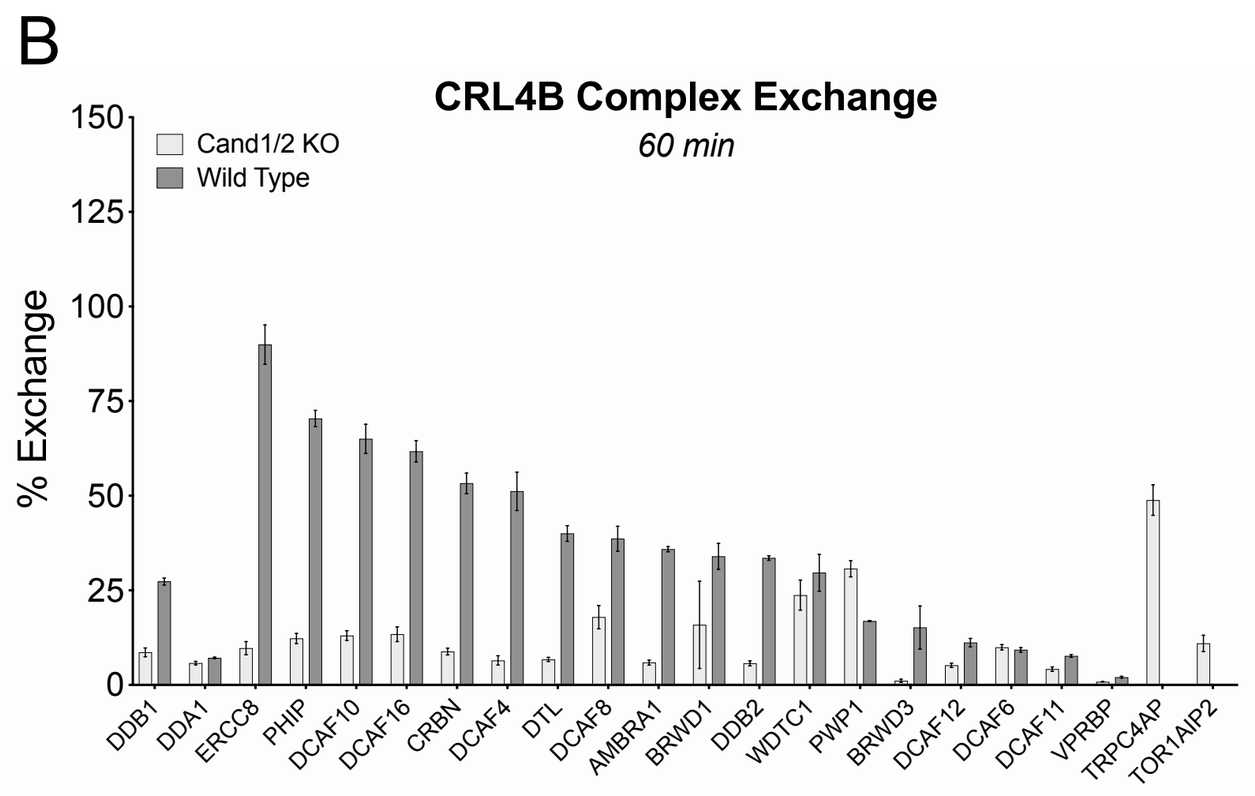

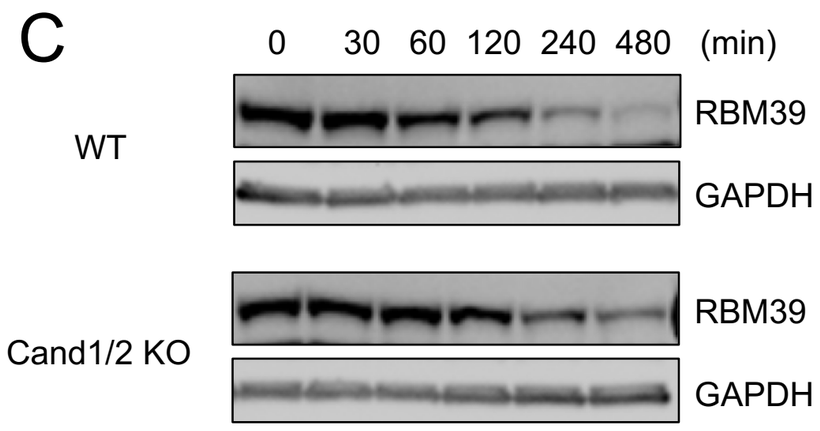

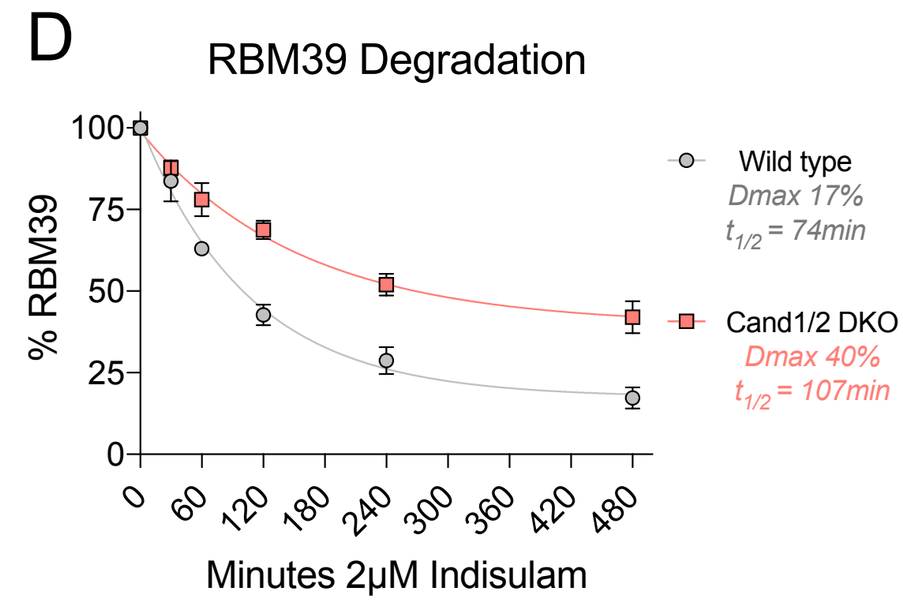

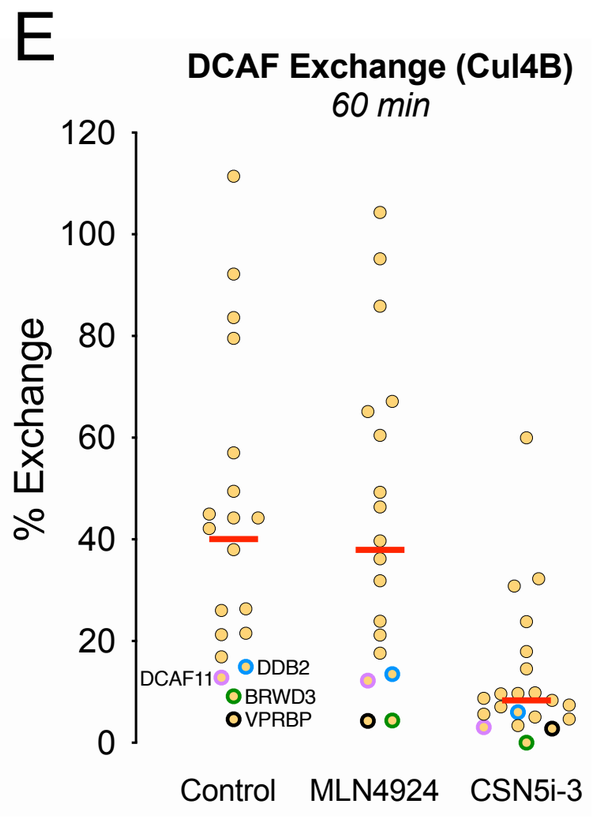

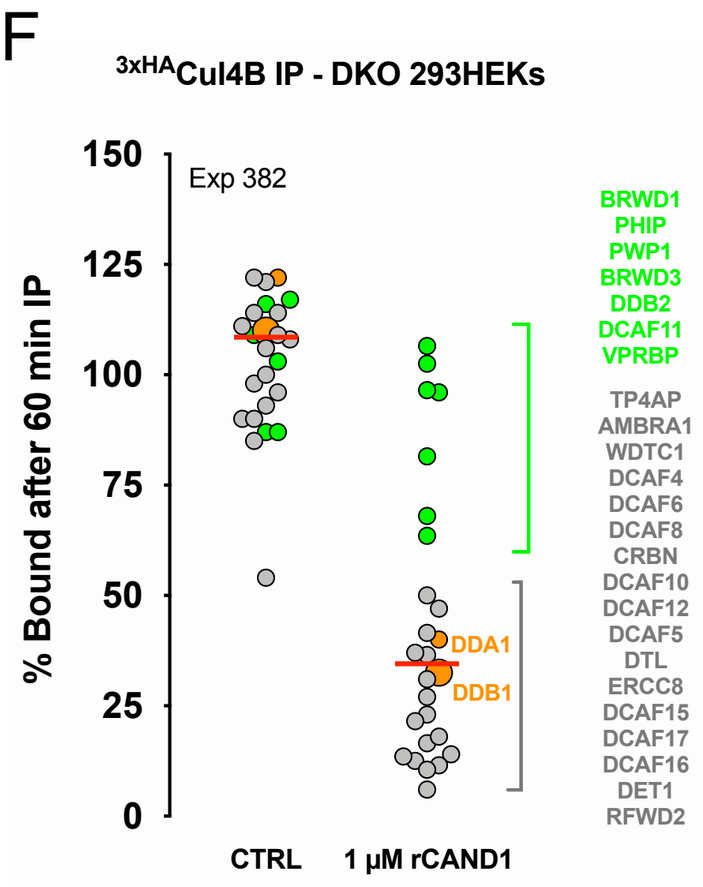

Figure Supplement 2. CRL4 complexes exchange DDB1•DCAFs via Cand1 and are stabilized by CSN5i-3 and Molecular Sponge, Related to Figure 2. (A) 293T/17$^{3xHA-Cul4B}$ cells were grown in heavy medium and 293T/17 WT cells in light medium, harvested and mixed at a ratio of 1:1, followed by lysis and anti-HA immunoprecipitation for different periods of time as well as LC-MS analysis. SILAC ratios of Cul4-binding proteins of ~1 translate to 100% exchange. This data is displayed as a dot-plot in Figure 2B. (B) Flp-In T-REx HEK293$^{3xHA-Cul4B}$ Cand1/2 double knock out (DKO) cells were grown in light medium and Flp-In T-REx HEK293 DKO cells in heavy medium and processed as for (A). This data is displayed as a dot-plot in Figure 2C. (C- D) Flp-In T-REx HEK293$^{3xHA-Cul4B}$ Cand1/2 double knock out (DKO) and wild type cells were treated with 2μM indisulam for indicated times, lysed in 2x LDS buffer and processes for quantitative western blotting. Shown is one representative replicate of n = 4, data was plotted and fitted to a single exponential to yield $t_{1/2}$. (E) 293T/17$^{3xHA-Cul4B}$ cells were grown in heavy medium and 293T/17 WT cells in light medium, either pre-treated with 1μM MLN4924 or 1μM CSN5i-3 for 4h and processes as for (A). (F) Flp-In T-REx HEK293$^{3xHA-Cul4B}$ Cand1/2 double knock out (DKO) cells were grown in light medium, lysed and immunoprecipated via anti-HA resin and either exposed to lysis buffer or lysis buffer with 1μM Cand1 and incubated for 60min under rotation at 4C. Bead-bound complexes were then washed and processed for PRM LC-MS analysis. Error bars represent the main ± SEM.

Figure S3 (related to Figure 3)

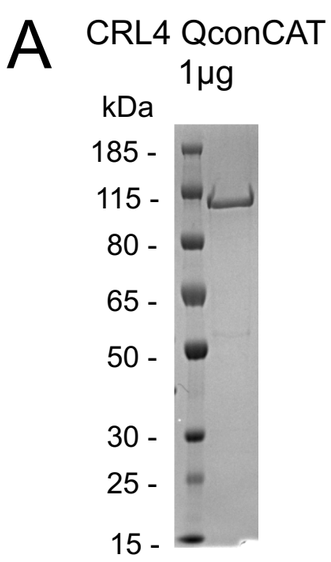

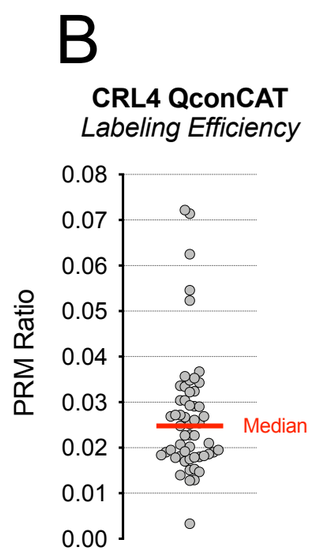

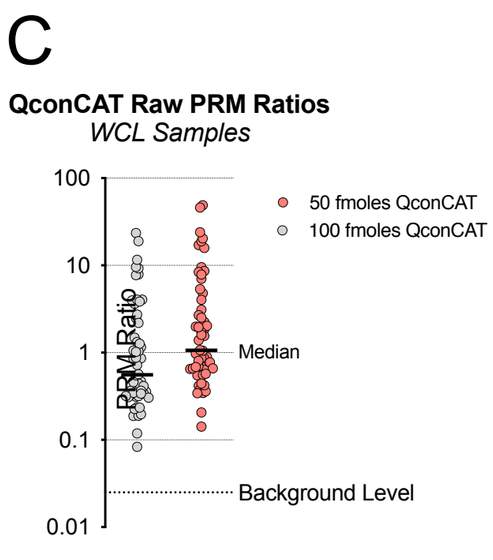

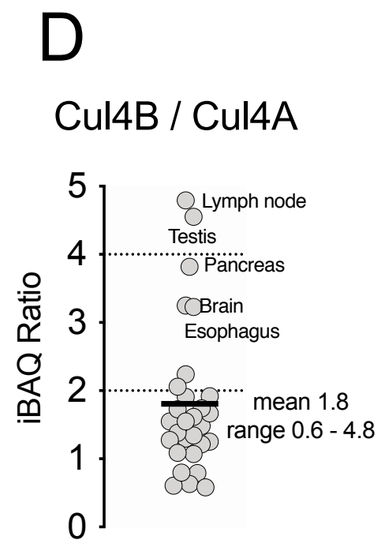

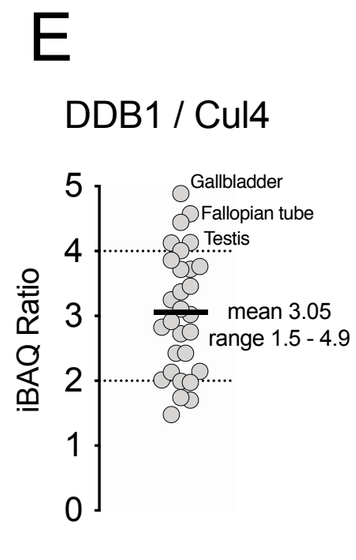

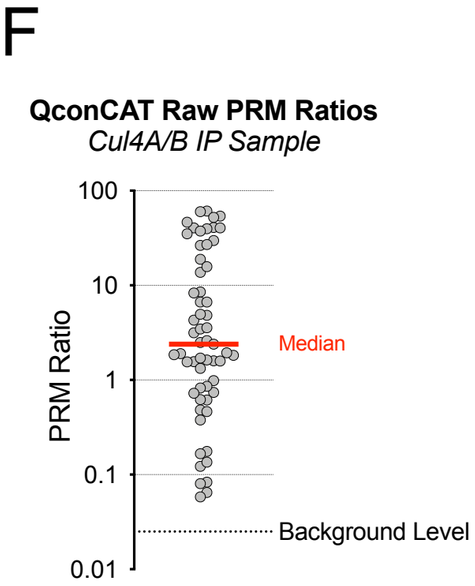

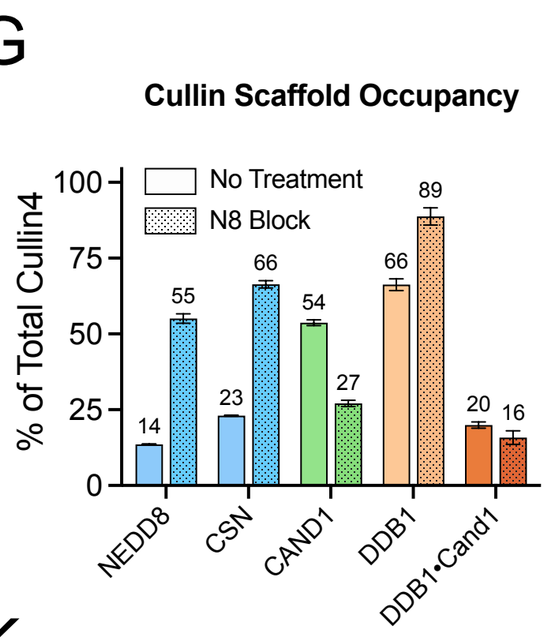

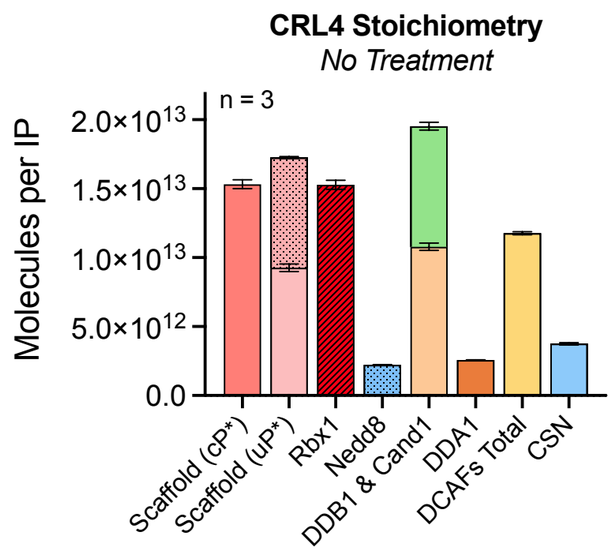

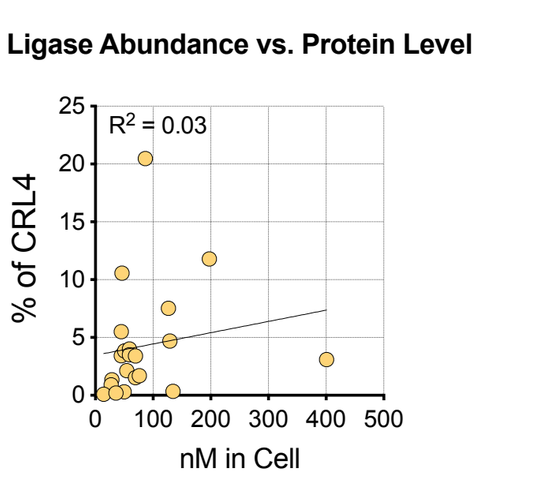

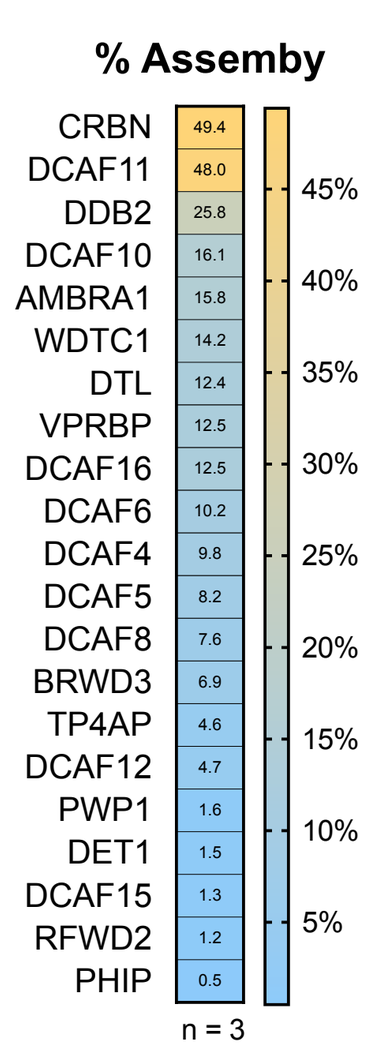

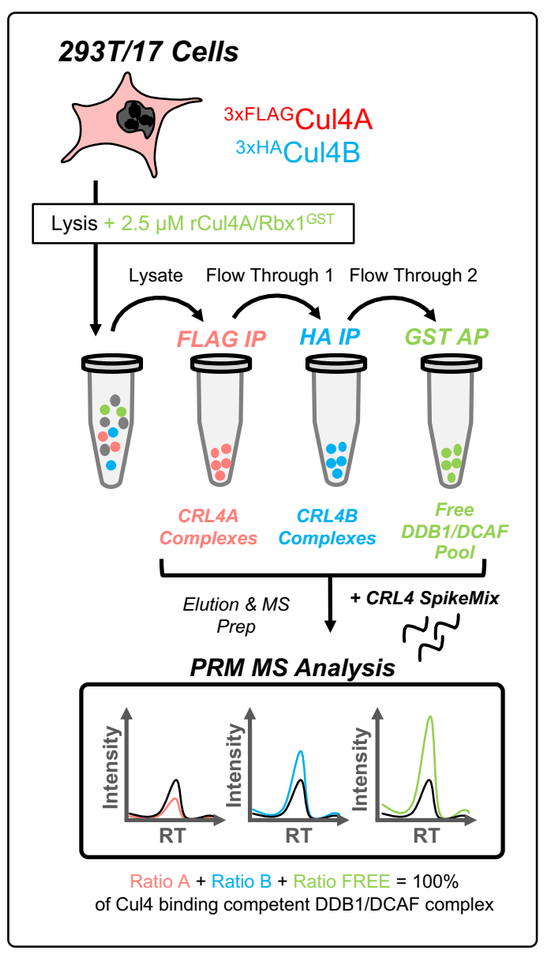

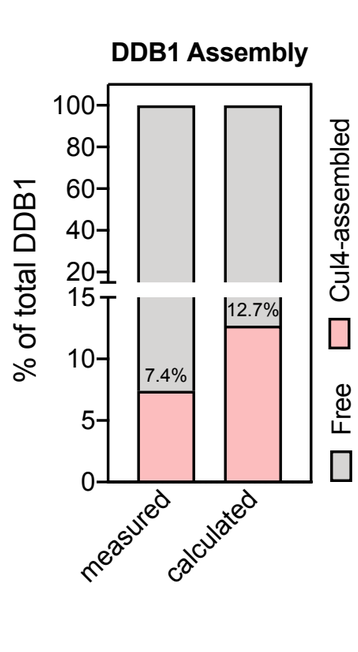

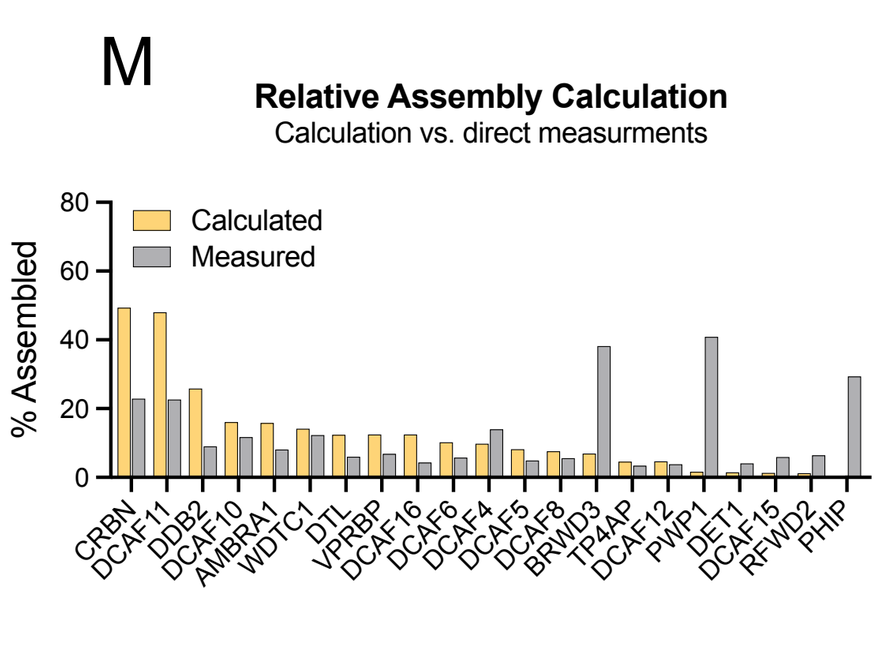

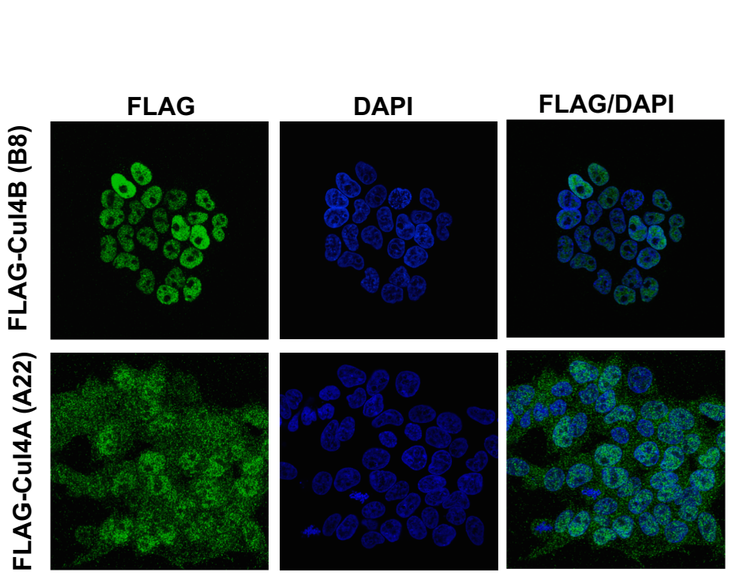

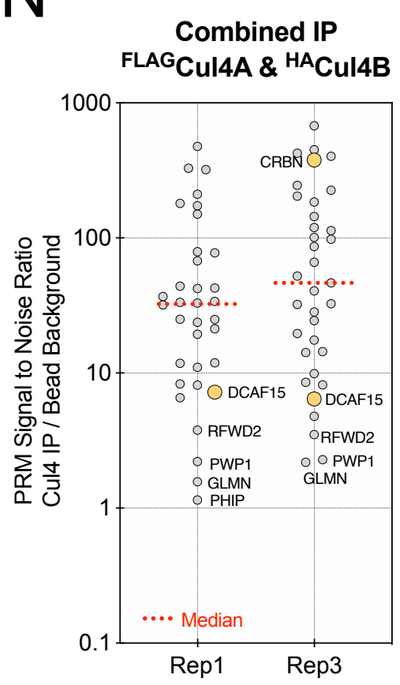

Figure Supplement 3. Individual CRL4 ligases show Cullin-scaffold preferences and differ up to 200-fold in absolute abundance, Related to Figure 3. (A) Coomassie stained SDS-PAGE gel of 1µg CRL4 QconCAT standard. (B) CRL4 QconCAT protein was digested with trypsin and analysis via PRM MS to determine the labeling efficiency. (C) 293T/17$^{3xFLAG\text{-}Cul4A\ \&\ 3xHA\text{-}Cul4B}$ cells were lysed in 8M Urea, spiked with CRL4 QconCAT protein standard followed by tryptic digest and PRM LC-MS analysis. Heavy to Light ratios were converted to nM cellular concentrations as described in the methods section. Shown in (C) are the PRM ratios measured for the experiment displayed in Figure 3B. The spiked concentration of the QconCAT standard was chosen so that all PRM ratios measured were well beyond the ~2% background signal. (D-E) iBAQ values for the indicated proteins were extracted from Wang et al. 2019 and Cul4B/Cul4A ratios as well as DDB1/Cul4 Ratios calculated and plotted. (F) CRL4 complexes were immunopurified from 293T/17$^{3xFLAG\text{-}Cul4A\ \&\ 3xHA\text{-}Cul4B}$ cells pulsed N8 Block (5min 1µM CSN5i-3 & 1µM MLN4924) via combined anti-HA and anti-FLAG IP, eluates spiked with CRL4 QconCAT protein standard and analyzed via PRM LC-MS. Shown are the PRM ratios measured for the experiment displayed in Figure 3C. (G) Occupancies of the Cul4 scaffold by various proteins as calculated from experiments displayed in Figure 3B, C. (H) CRL4 stoichiometries as measured for a Cul4 IP sample from cells where post-lysis exchange was not inhibited. (I) Correlation plot of cellular concentrations of DCAFs and their overall % representation within all captured CRL4 complexes. (J) Percent Assembly (Percent of DCAF bound to Cul4 versus free) of each DCAF as calculated from stoichiometry data. (K) 293T/17$^{3xFLAG\text{-}Cul4A\ \&\ 3xHA\text{-}Cul4B}$ cells were pulsed with N8 Block and lysed in the presence of 2.5 µM rCul4A•Rbx1^{GST} molecular sponge followed by sequential immunoprecipation via anti-FLAG, anti-HA and GSH resin to capture assembled CRL4 complexes or free DDB1•DCAF modules. IP-eluates were digested, spiked with CRL4 SpikeMix peptide standard and analyzed via PRM LC-MS. (L) Percent Assembly of DDB1 as measured via (K) or calculated from stoichiometries and cellular concentrations. (M) comparing Percent Assembly for all assessed DCAF proteins as measured in (K) or calculated from stoichiometries and concentrations. (N) Lysates from 293T/17$^{3xFLAG\text{-}Cul4A\ \&\ 3xHA\text{-}Cul4B}$ or 293T/17 wild type cells were immunoprecipitated with either anti-FLAG or anti-HA resin and eluates spiked with CRL4 SpikeMix followed by PRM analysis. PRM ratios obtained from CRL4 IPs were then related to PRM ratios obtained from bead background samples to derive the displayed signal to noise ratios. (O) 293T/17$^{3xFLAG\text{-}Cul4A}$ and 293T/17$^{3xFLAG\text{-}Cul4B}$ cells were fixed on a cover slip and stained with anti-FLAG antibodies followed by microscopic analysis. In all figures, error bars represent the mean ± SEM.

Figure S4 (related to Figure 4)

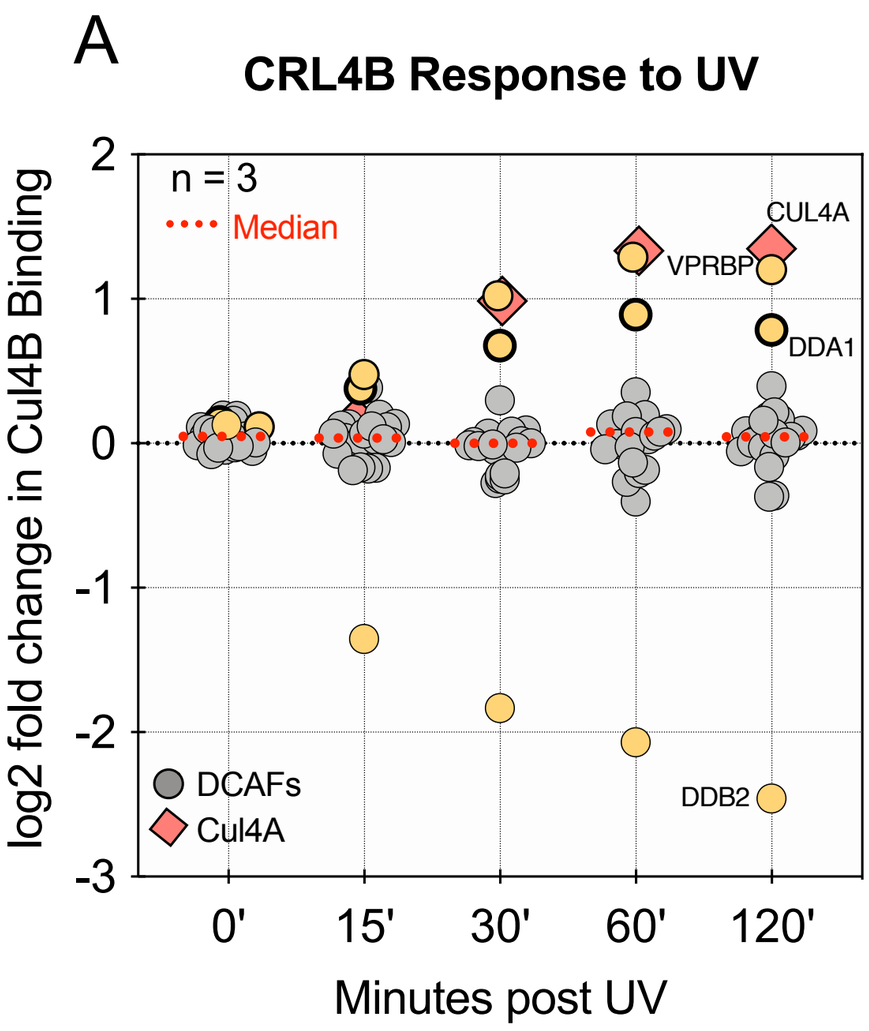

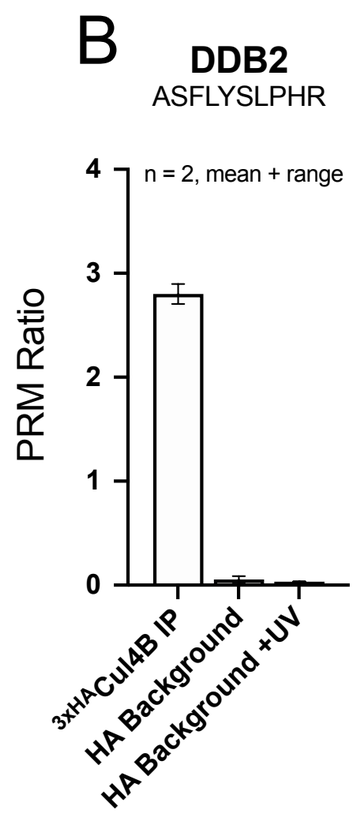

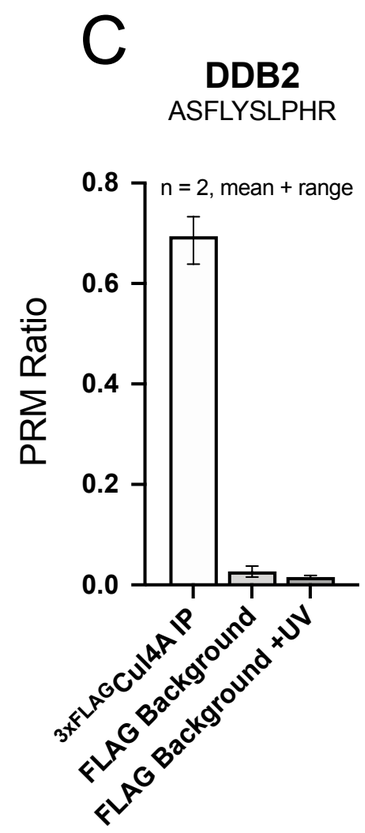

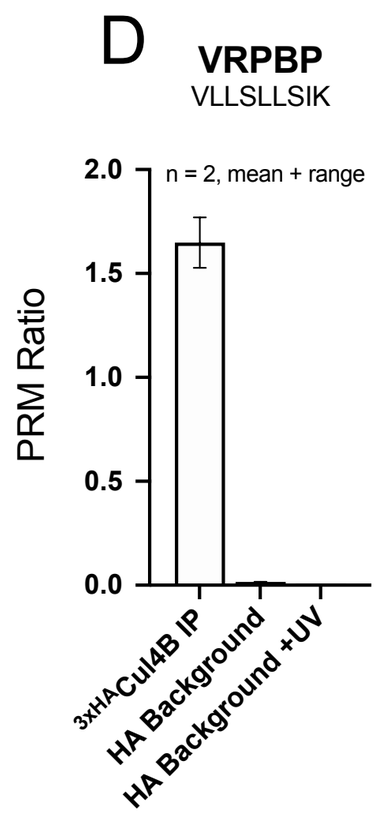

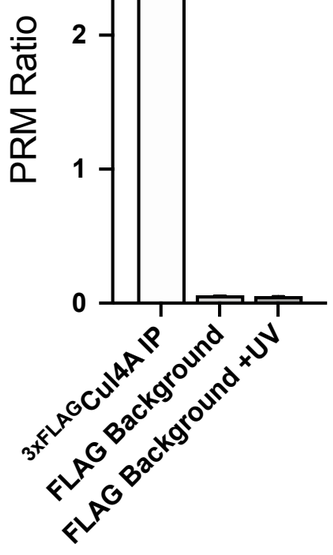

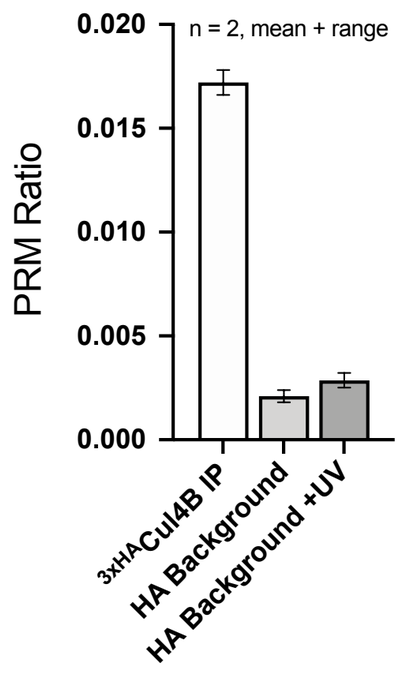

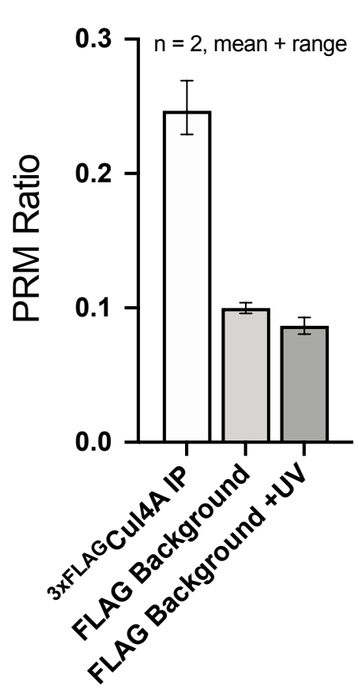

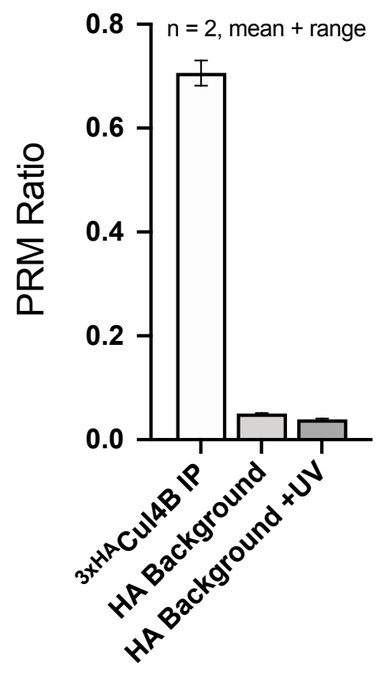

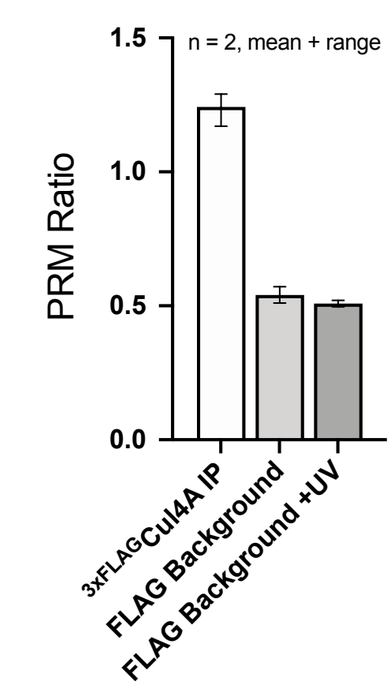

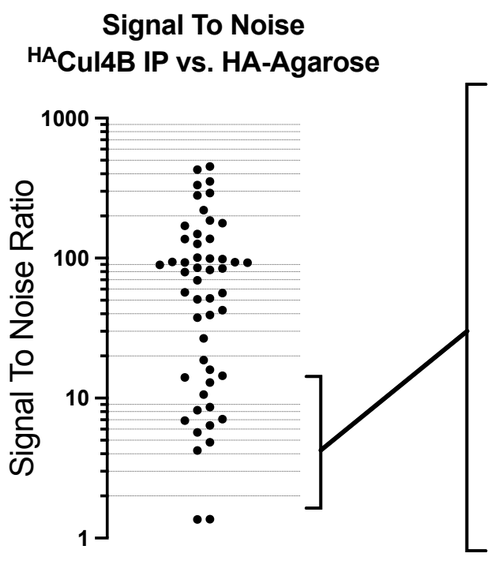

Peptide with S/N < 20	Signal/Noise
TFNEPESVIAR _ BRWD1	19
FNLILADTNSDR _ DCAF4	16
VVVDPVVTEQPSTSSAAK _ PHIP	14
DQEQVELEGESSAPPR _ DDA1	14
YGIINLQSLK _ DCAF4	13
GLPVYNK _ DDA1	11
DSPPASEAPASEPGYVNYTK _ DCA15	9
LPDNYTQDTWR _ CUL4A	8
IIHVGPNQVK _ DCA17	7
YTSEDVVTLR _ DET1	7
TASQLDEFQECLSK _ RFWD2	6
TLLASTHVNHNIYITEVK _ AMRA1	6
TVGVAFNQETGHWER _ AMRA1	5
TAVSCLSQNDWK _ DCNL1	4
NSSISGPFGSR _ PWP1	1
SVALYDCR _ PWP1	1

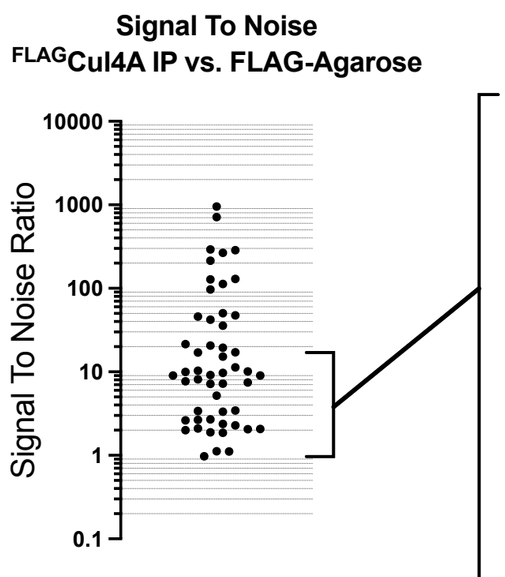

Peptide with S/N < 20	Signal/Noise
TPSSSPPITPPASETK_DTL	19
QVCPLDNR_RBX1	17
TFNEPESVIAR_BRWD1	17
LAFLDPISGK_BRWD3	15
YLAIAPPIIK_DDB1	11
NENVLTVTASGR_DCAF17	10
WSGIPQLLLK_TP4AP	10
TLLATGGDNPNSLAIYR_DCAF12	10
DGETSLVTGEADEGR_DCAF5	10
NATLHSEVQFPCSASSNNFAR_DET1	9
GTWLASGSDDLK_DCAF8	9
GGSYPHLLWDVR_DCAF6	9
NTITVPASFMLR_DCAF6	8
TAVSCLSQNDWK_DCNL1	8
YTSEDVVTLR_DET1	7
LTHYIEEANVGR_DCAF10	7
HGLGAGLGGPGAR_DCAF10	7
VHVHDLTVK_WDTC1	5
DSPPASEAPASEPGYVNYTK_DCAF15	3
EAFETFINK_CUL4B	3
VVVDPVVTEQPSTSSAAK_PHIP	3
IWAPTAEASTELTGLK_DCAF8	3
ISGQLSPR_DCAF15	3
TLSHNLLVSEVYNQLK_CUL4B	3
DQEQVELEGESSAPPR_DDA1	2
FNLILADTNSDR_DCAF4	2
GLPVYNK_DDA1	2
YGIINLQSLK_DCAF4	2
TLLASTHVNHNIYITEVK_AMBRA1	2
TVGVAFNQETGHWER_AMBRA1	2
TASQLDEFQECLSK_RFWD2	2
LINEGDVPHLPVNR_BRWD3	2
NSSISGPFGSR_PWP1	1
SVALYDCR_PWP1	1
IMASLNLLR_GLMN	1

Figure Supplement 4. CRL4s reshape their assemblies and form Cul4A•Cul4B dimers upon UV-induced DNA damage, Related to Figure 4. (A) 293T/17$^{3xHA\text{-}Cul4B}$ cells were exposed to UV light at a dose of 50 J/m^2 and lysed indicated time points followed by anti-HA immunoprecipitation and PRM MS analysis. Displayed is data from Figure 4B as a dot plot. (B-I) Background signal assessment for individual proteins in Figure 4B. Untagged wild type 293T/17 cells were either treated or not with 50 J/m^2 UV light followed by lysis and incubation with anti-HA resin followed by PRM MS analysis. (J & K) Dot plot of signal to noise ratios as computed from measured PRM ratios in a HA-Cul4B IP sample or a FLAG-Cul4A IP sample divided by measured PRM ratios in a HA or FLAG background sample. In all figures, error bars represent the mean ± SEM.

Figure S5 (related to Figure 5)

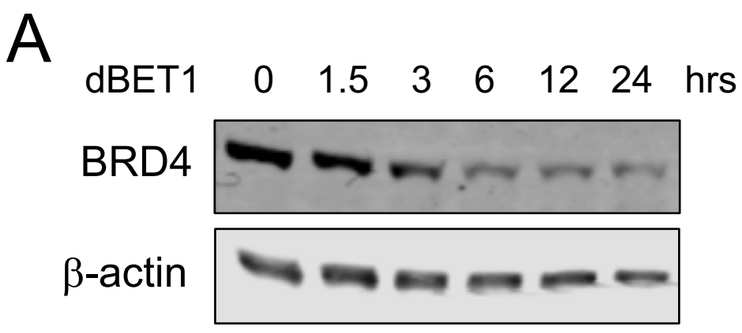

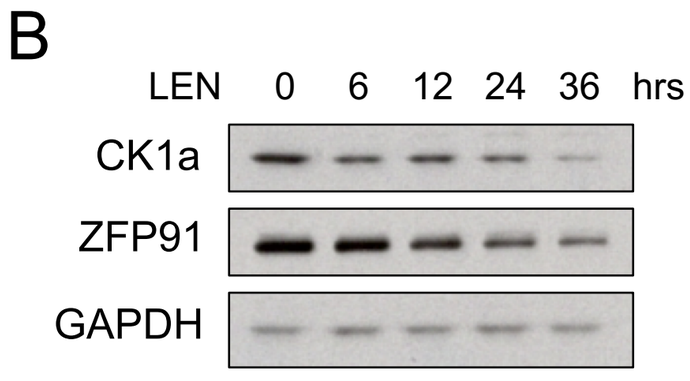

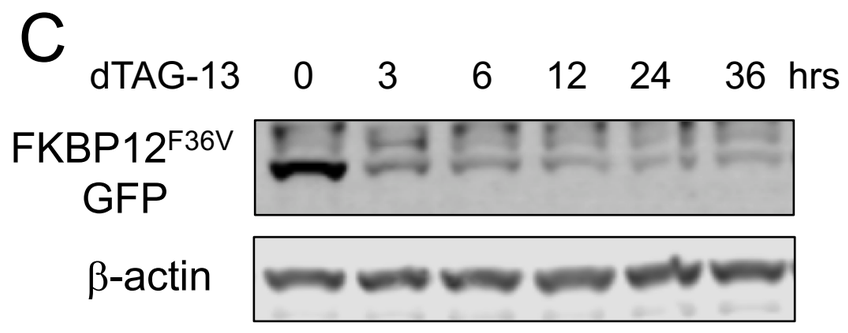

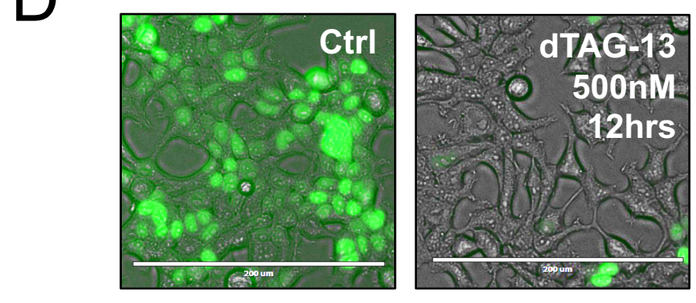

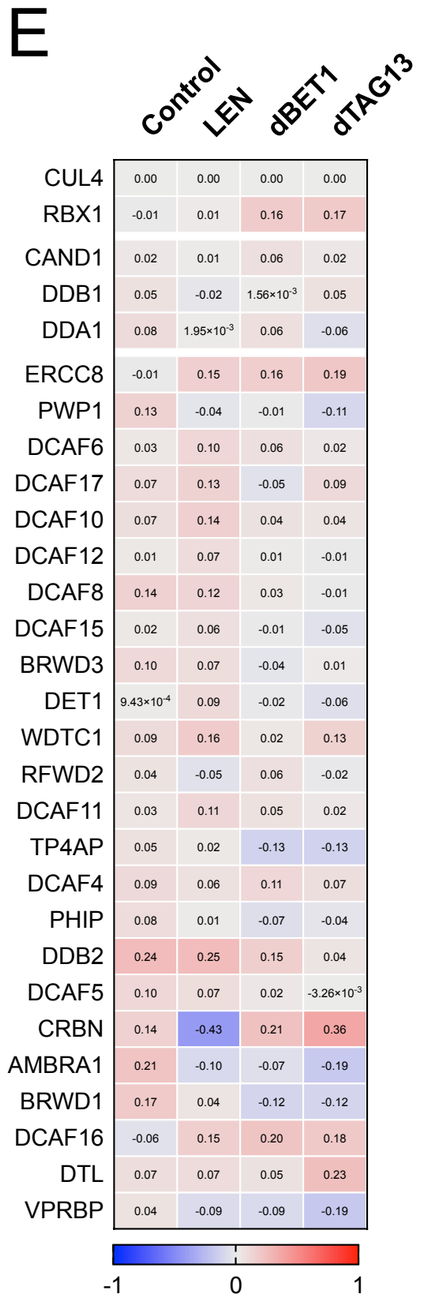

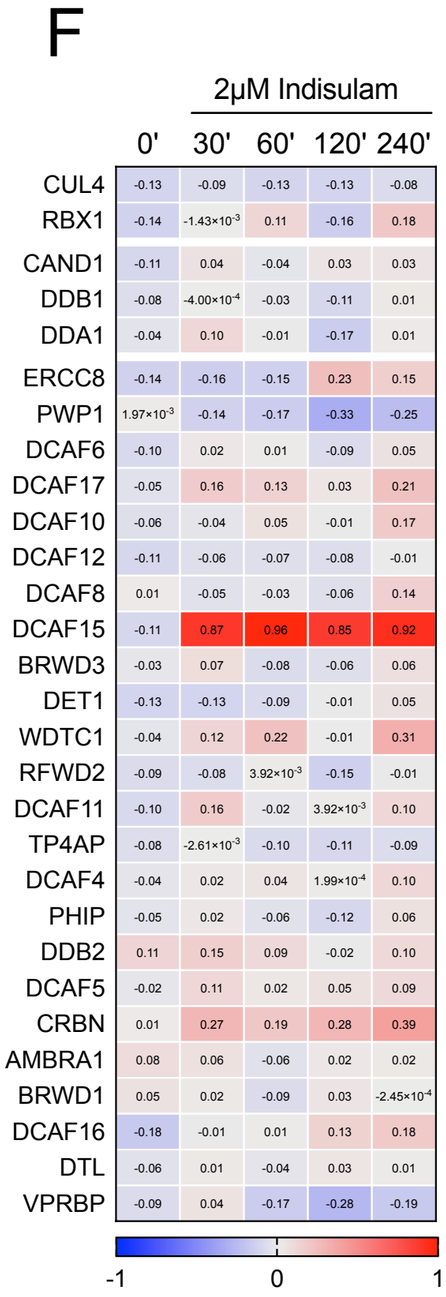

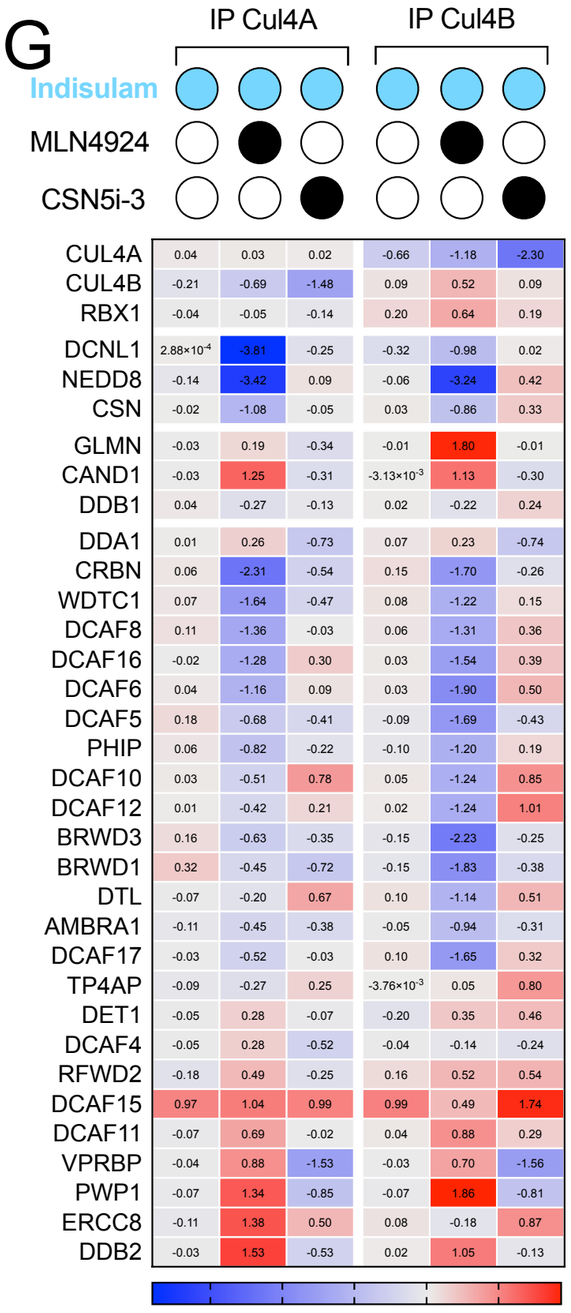

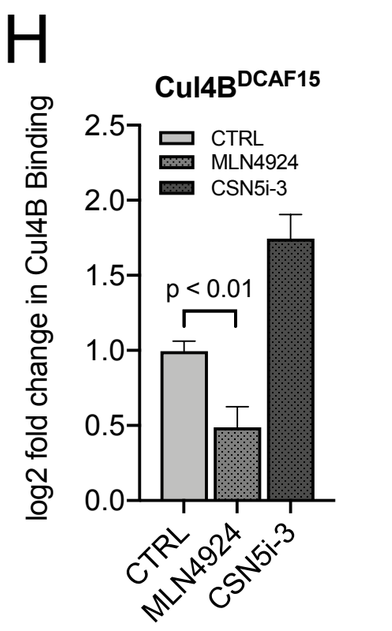

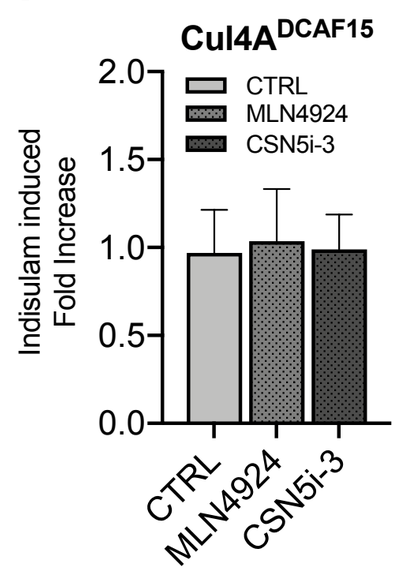

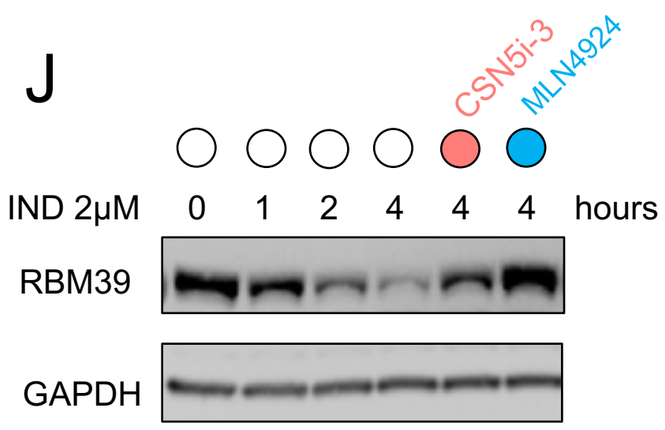

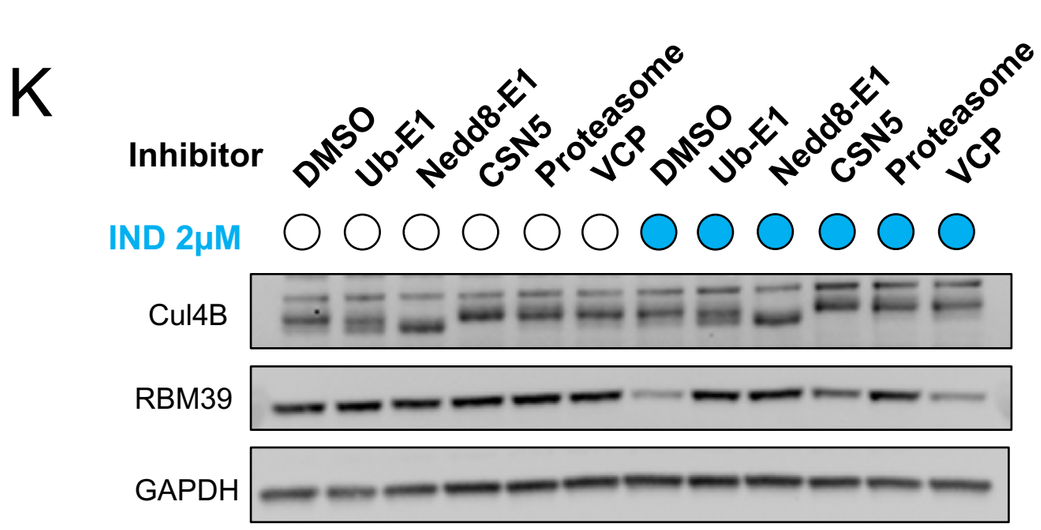

3h co-treatment – MLN7243 1μM, MLN4924 1μM, CSN5i-3 1μM, BTZ 5μM, CB5083 5μM

Figure Supplement 5. CRL4s reshape their assemblies and form Cul4A•Cul4B dimers upon UV-induced DNA damage, Related to Figure 5. (A-B) 293T/17 cells were treated with (A) 100nM dBET1 or (B) 30μM Lenalidomide for indicated times, lysed in SDS sample buffer followed by SDS Page and western blot. Displayed is one representative replicate. (C- D) 293T/17$^{3xFLAG\text{-}Cul4A\ \&\ 3xHA\text{-}Cul4B}$ cells stably over-expressing FKBP12^{F36V}-GFP were treated with (C) 500nM dTAG-13 for indicated times, lysed in SDS sample buffer followed by SDS-PAGE and western blotting or (D) treated for 12 hours and imaging of GFP-fluorescence signal per light microscope. Displayed is one representative replicate. (E) 293T/17$^{3xFLAG\text{-}Cul4A\ \&\ 3xHA\text{-}Cul4B}$ cells were treated for 1 hour with 30μM Lenalidomide, 100nM dBET1 or 500nM dTAG-13, pulsed with N8 Block before harvest. Lysates were immunoprecipitated with anti-HA and anti-FLAG resin to capture CRL4 complexes followed by PRM LC-MS analysis. Heatmap for data displayed in Figure 5H and 5I. (F) 293T/17$^{3xFLAG\text{-}Cul4A\ \&\ 3xHA\text{-}Cul4B}$ cells were treated with 2μM Indisulam for the indicated times, pulsed with N8 Block and lysates immunoprecipitated for via anti-HA and anti-FLAG to capture CRL4 complexes followed by PRM LC-MS. Heatmap for data displayed in Figure 5J and 5K. (G) 293T/17$^{3xFLAG\text{-}Cul4A\ \&\ 3xHA\text{-}Cul4B}$ cells were pre-treated or not with 1μM MLN4924 or 1μM CSN5i-3 for 30 min followed by treatment with 2μM Indisulam for 60 min, pulsed with N8 Block and lysates immunoprecipitated for either via anti-FLAG or anti-HA to capture CRL4A and CRL4B complexes individually, followed by PRM LC-MS. (H, I) Bar graphs of log2 fold changes of DCAF15 bound to Cul4B and Cul4A for data displaye din heatmap (G). (J) 293T/17$^{3xFLAG\text{-}Cul4A\ \&\ 3xHA\text{-}Cul4B}$ cells were treated with 2μM indisulam for indicated times with or without co-treatment of MLN4924 or CSN5i-3 followed by lysis in 2x SDS sample buffer and SDS-PAGE as well as western blotting. (K) 293T/17$^{3xFLAG\text{-}Cul4A\ \&\ 3xHA\text{-}Cul4B}$ cells were treated with 2μM indisulam for 3 hours with or without co-treatment of 1μM ubiquitin E1 inhibitor MLN7243, 1μM Nedd8 E1 inhibitor MLN4924, 1μM CSN inhibitor CSN5i-3, 5μM proteasome inhibitor Bortezomib or 5μM p97/VCP inhibitor CB5083, followed by lysis in 2x SDS sample buffer and SDS-PAGE as well as western blotting. In all figures, error bars represent the mean ± SEM.

Figure Supplement 6 (related to Figure 5,6)

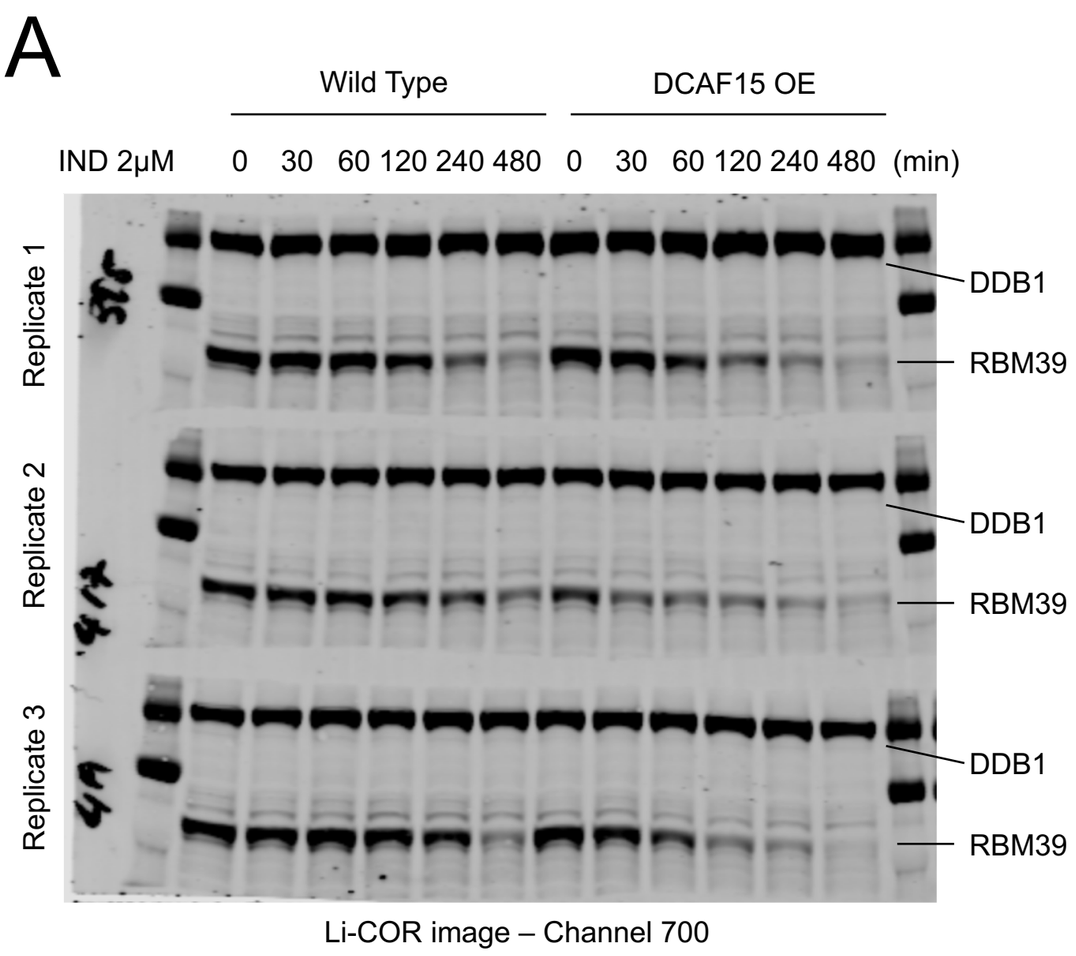

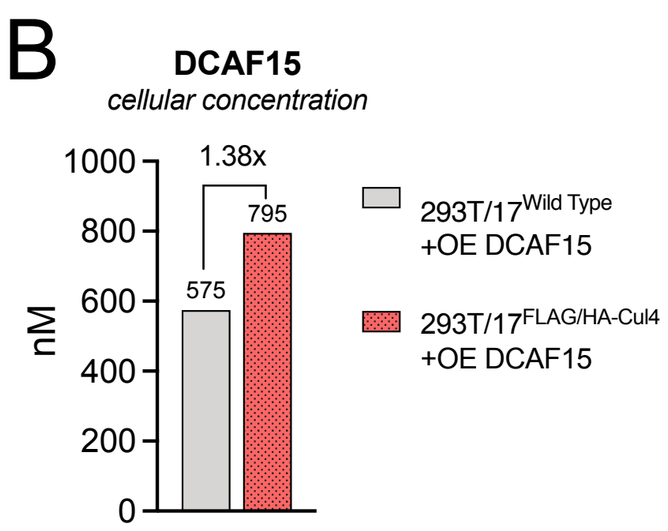

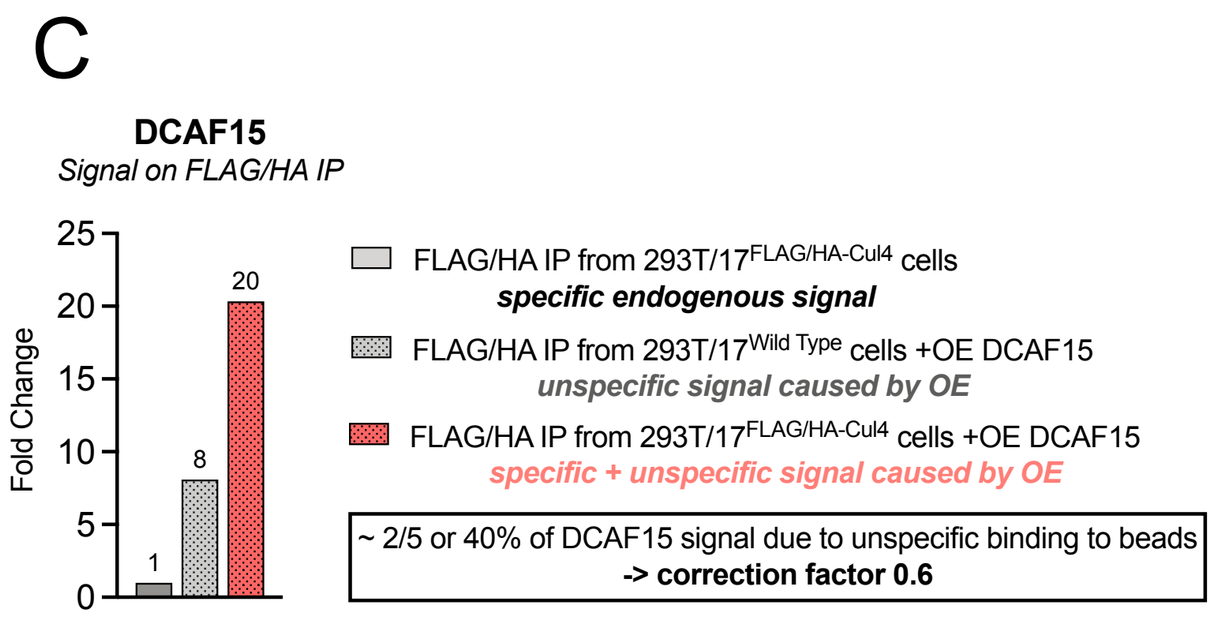

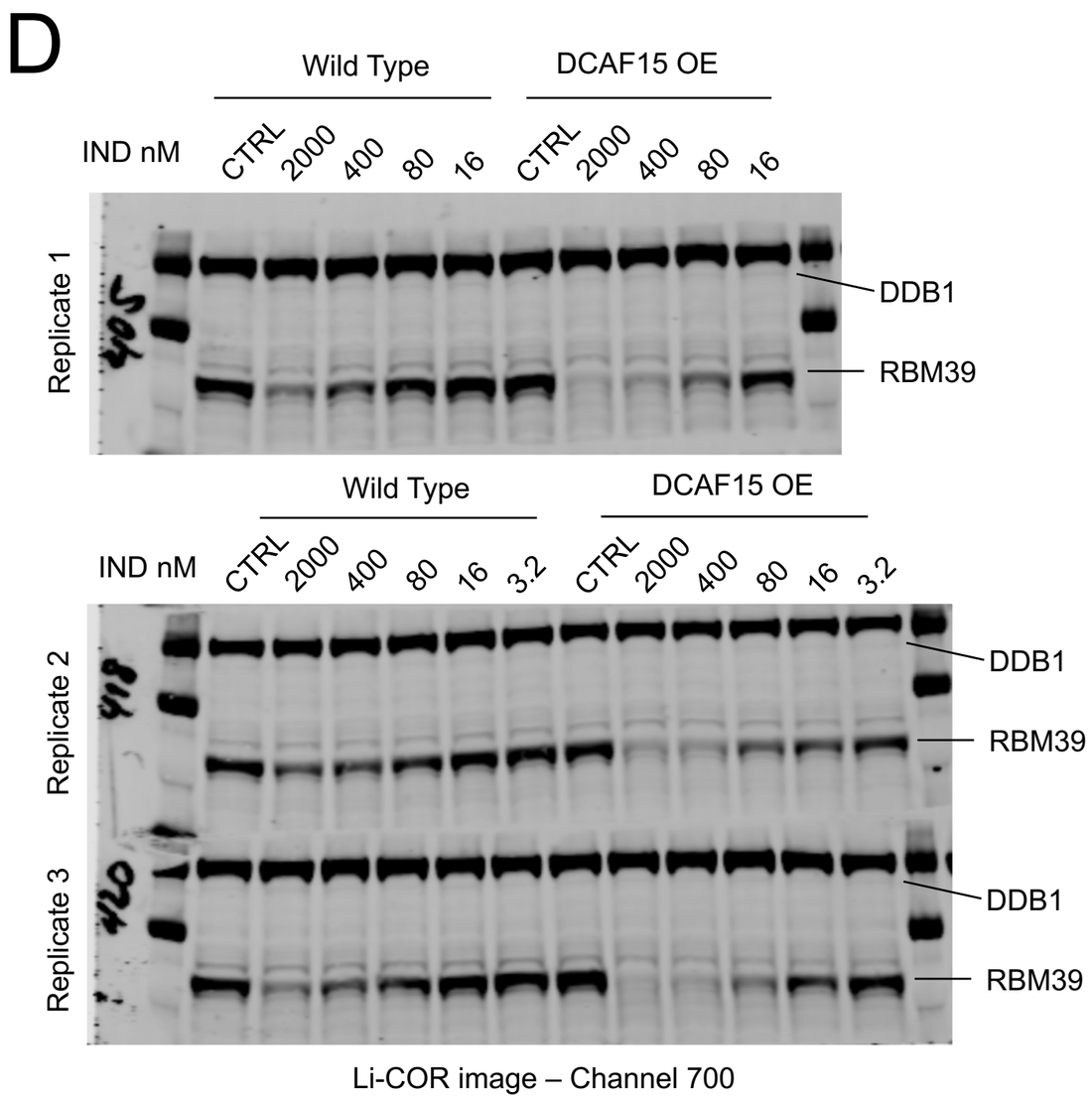

Figure Supplement 6. Higher DCAF expression can result in faster substrate degradation via increased substrate occupancy, Related to Figure 5,6 (A) 293T/17$^{3xFLAG\text{-}Cul4A\ \&\ 3xHA\text{-}Cul4B}$ wild type or DCAF15 over-expressing cells were treated with 2μM indisulam for indicated times, lysed in 2xSDS sample buffer and processed via SDS-PAGE for western blotting. (C) 293T/17 and 293T/17$^{3xFLAG\text{-}Cul4A\ \&\ 3xHA\text{-}Cul4B}$ cells over-expressing DCAF15 were lysed in 8M urea and processed for CRL4 QconCAT PRM analysis to measure cellular concentrations. (D) Anti-HA resin was exposed to lysates from 293T/17$^{3xFLAG\text{-}Cul4A\ \&\ 3xHA\text{-}Cul4B}$ cells, 293T/17 cells over-expressing DCAF15 or 293T/17$^{3xFLAG\text{-}Cul4A\ \&\ 3xHA\text{-}Cul4B}$ cells over-expressing DCAF15 to evaluate the unspecific background binding of over-produced DCAF15 to Anti-HA resin. The measured PRM ratios were normalized to over-expressed DCAF15 levels. To correct for ~40% unspecific background signal, DCAF15 PRM ratios displayed in Figure 6E were corrected by a factor of 0.6. (D) 293T/17$^{3xFLAG\text{-}Cul4A\ \&\ 3xHA\text{-}Cul4B}$ wild type or DCAF15 over-expressing cells were treated with 3.2nM, 16nM, 80nM, 400nM or 2μM indisulam for 8 hours, lysed in 2xSDS sample buffer and processed via SDS-PAGE for western blotting.

Figure S7 (related to Figure 1)

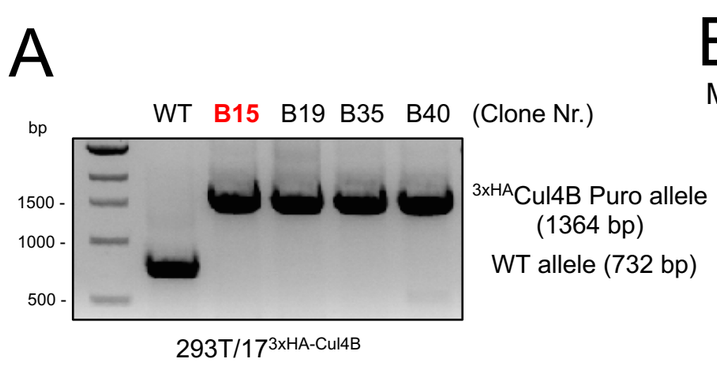

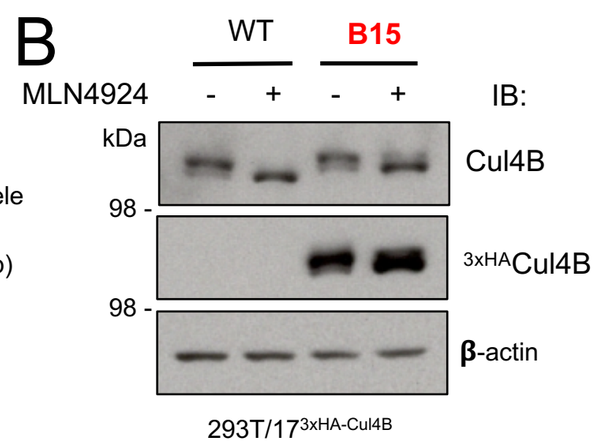

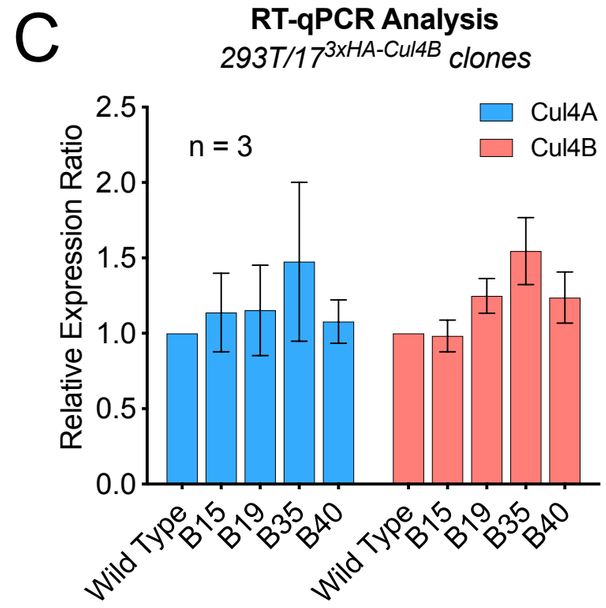

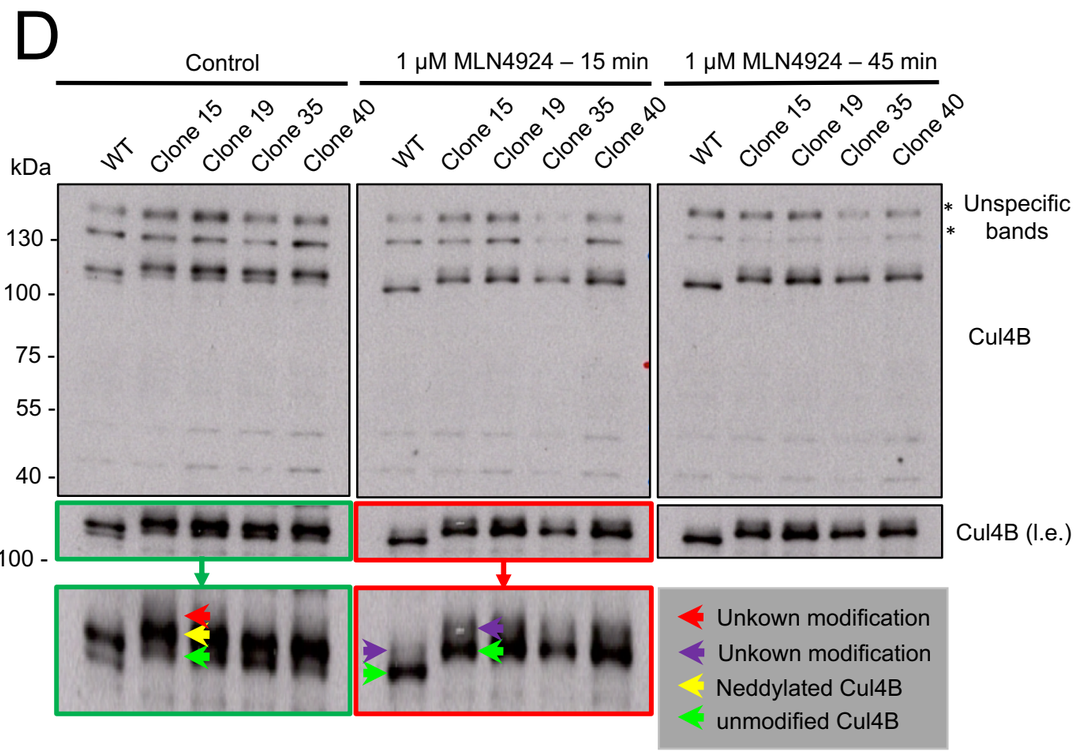

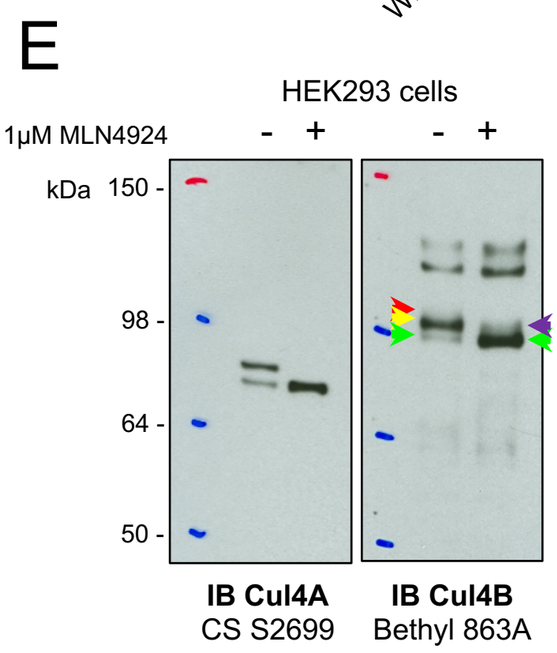

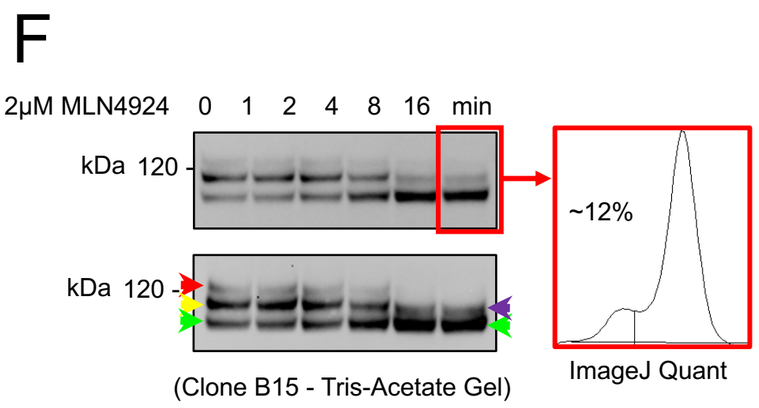

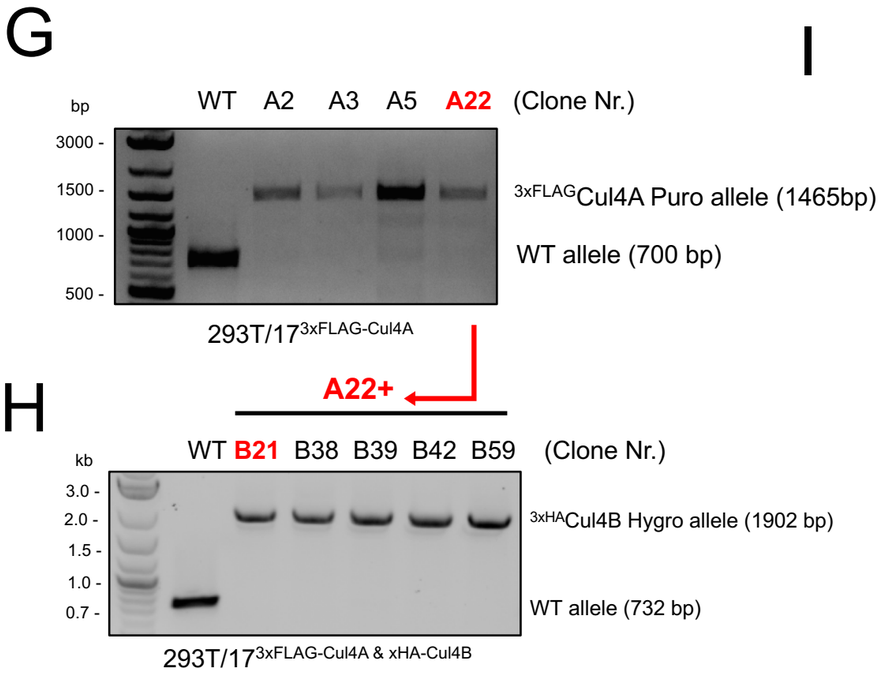

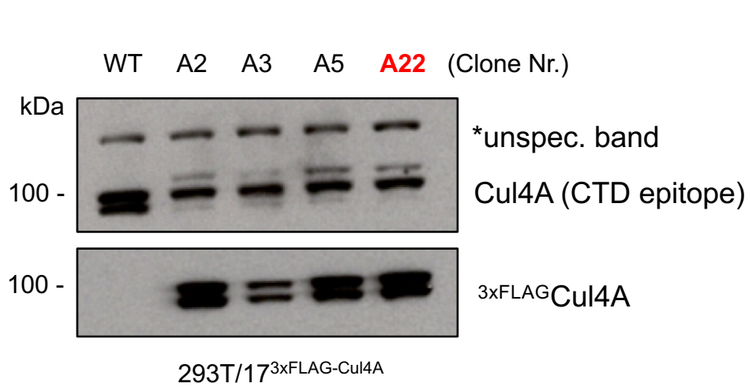

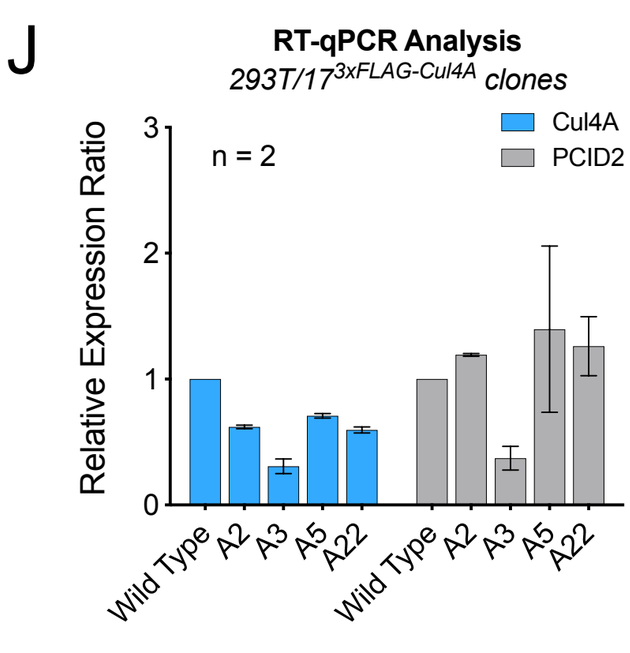

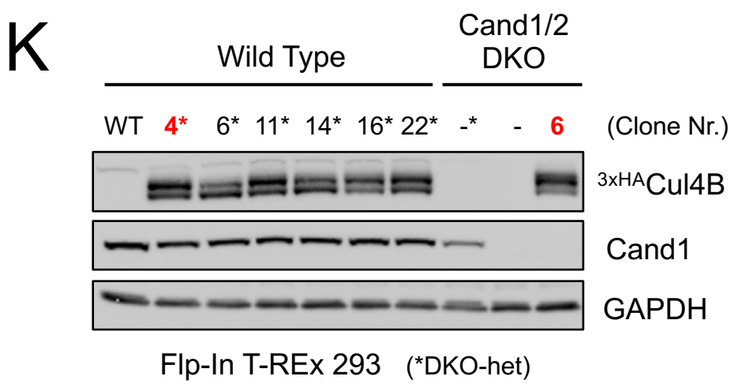

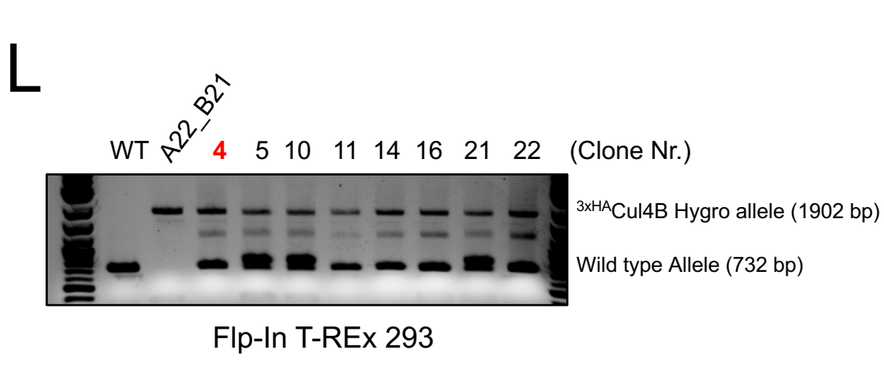

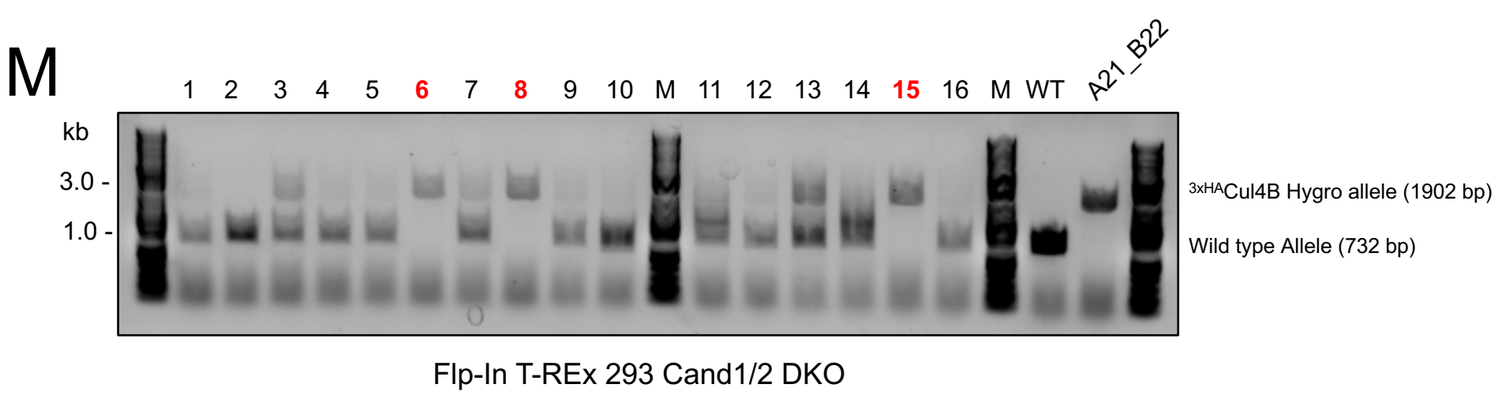

Figure Supplement 7. Genetic engineering of epitope tagged cell lines, Related to Figure 1. (A-C) Assessment of CRISPR/Cas9-engineered 293T/17$^{3xHA\text{-}Cul4B}$ single cell clones to (A)evaluate genomic insertion via PCR, (B) SDS-PAGE and western blotting to evaluate protein levels, as well as (C) quantitative RT-PCR to evaluate mRNA levels. (D-F) Monitoring of Cul4B and 3xHACul4B deneddylation in CRISPR/Cas9-engineered 293T/17$^{3xHA\text{-}Cul4B}$ single cell clones via MLN4924 treatment and SDS-PAGE followed by western blotting. Red arrows indicate Nedd8-Cul4B with unknown modification, purple band indicating Cul4B with unknown modification, yellow band indicating Nedd8-Cul4B and green band indicating unmodified Cul4B. (G-J) Assessment of CRISPR/Cas9-engineered 293T/17$^{3xFLAG\text{-}Cul4A}$ single cell clones using (G) genomic PCR, (I) SDS-PAGE and western blotting and (J) RT-qPCR. Western blotting for the FLAG-tag revealed successful integration and unaffected neddylation status. Therefore, the anti-Cu4A antibody against a C-terminal epitope likely does not associate well with the C-terminally neddyalted Cul4A. RT-qPCR of the essential gene PCID2 that is located upstream of Cul4A on chromosome 13 revealed normal levels for 3 out of 4 genes while Cul4A levels were slightly lower in clones carrying the insert. (H) Assessment of CRISPR/Cas9-engineered 293T/17$^{3xFLAG\text{-}Cul4A\ \&\ 3xHA\text{-}Cul4B}$ via genomic PCR. (K-M) Assessment of CRISPR/Cas9-engineered Flp-In T-REx HEK293$^{3xHA\text{-}Cul4B}$ wild type and Cand1/2 double knock out (DKO) single cell clones via (K) SDS-PAGE and western blotting and (L-M) genomic PCR. The clones marked in red in each figure were used for experiments in this study.

Figure S8 (related to Figure 1)

A

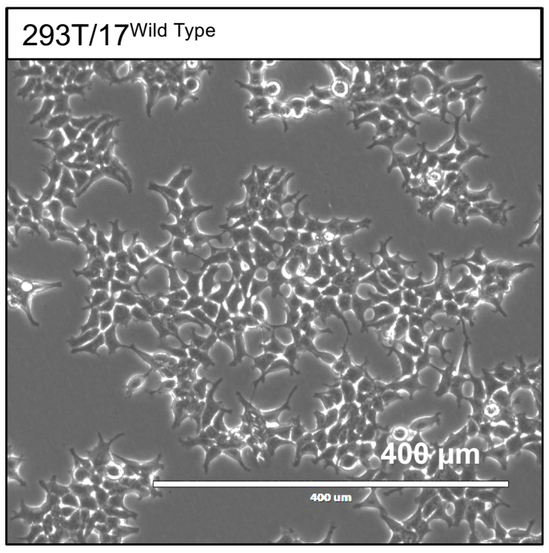

Wild Type Population – KR-7

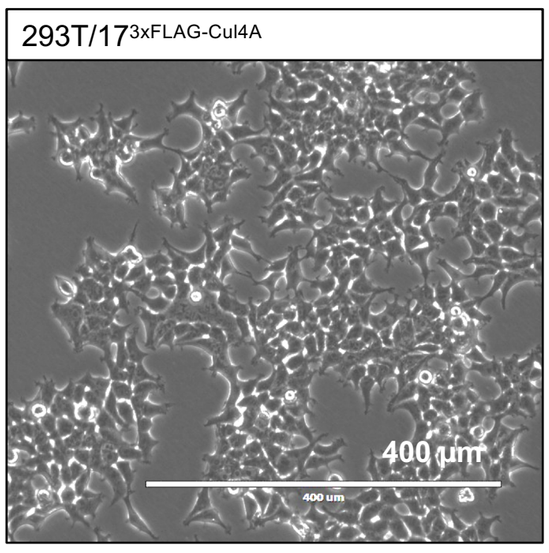

Clone A22 – KR-27

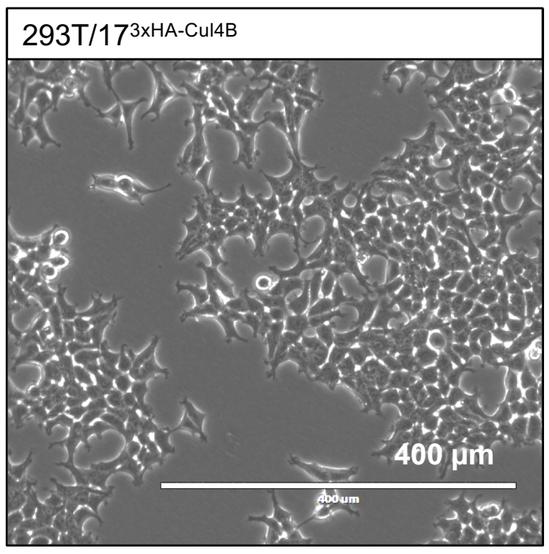

Clone B15 – KR-13

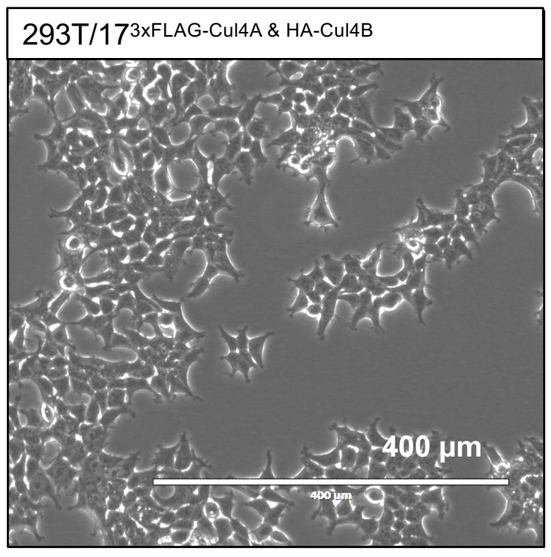

Clone A22_B21 – KR-52

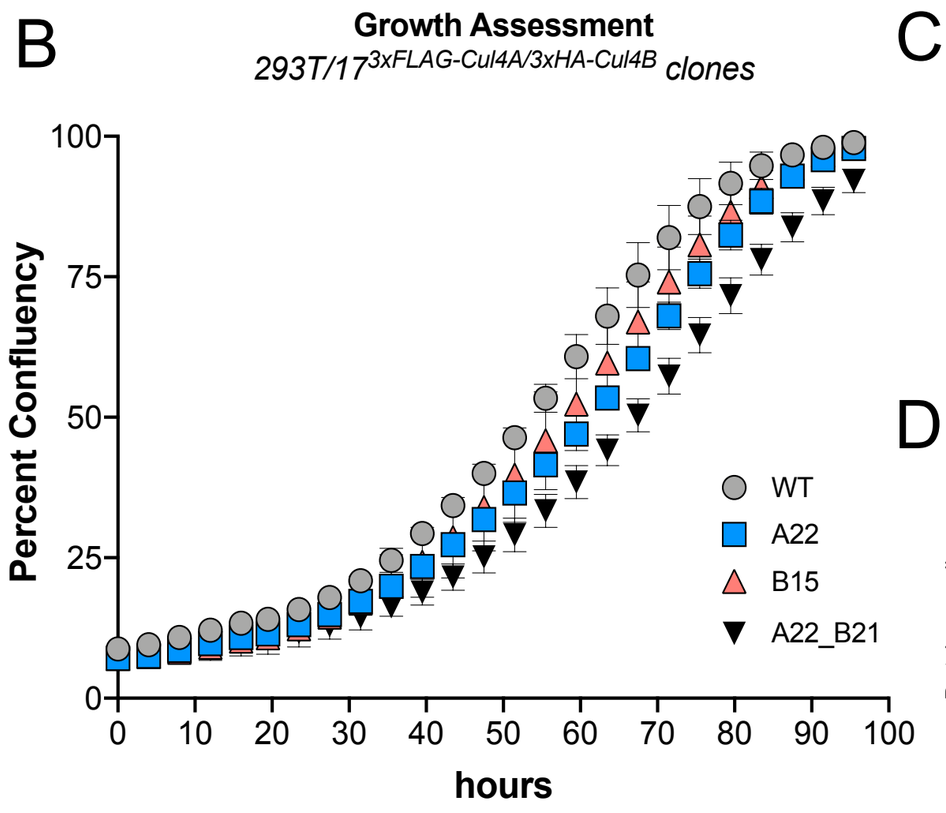

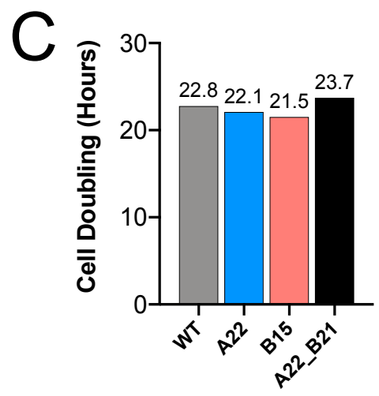

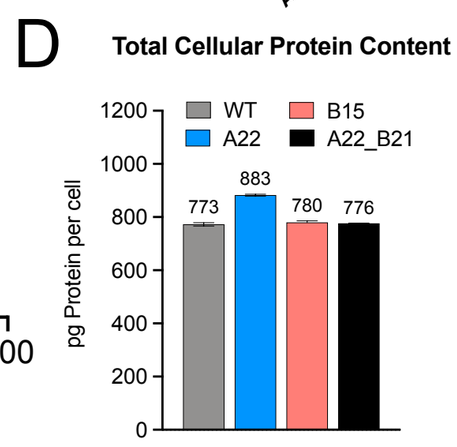

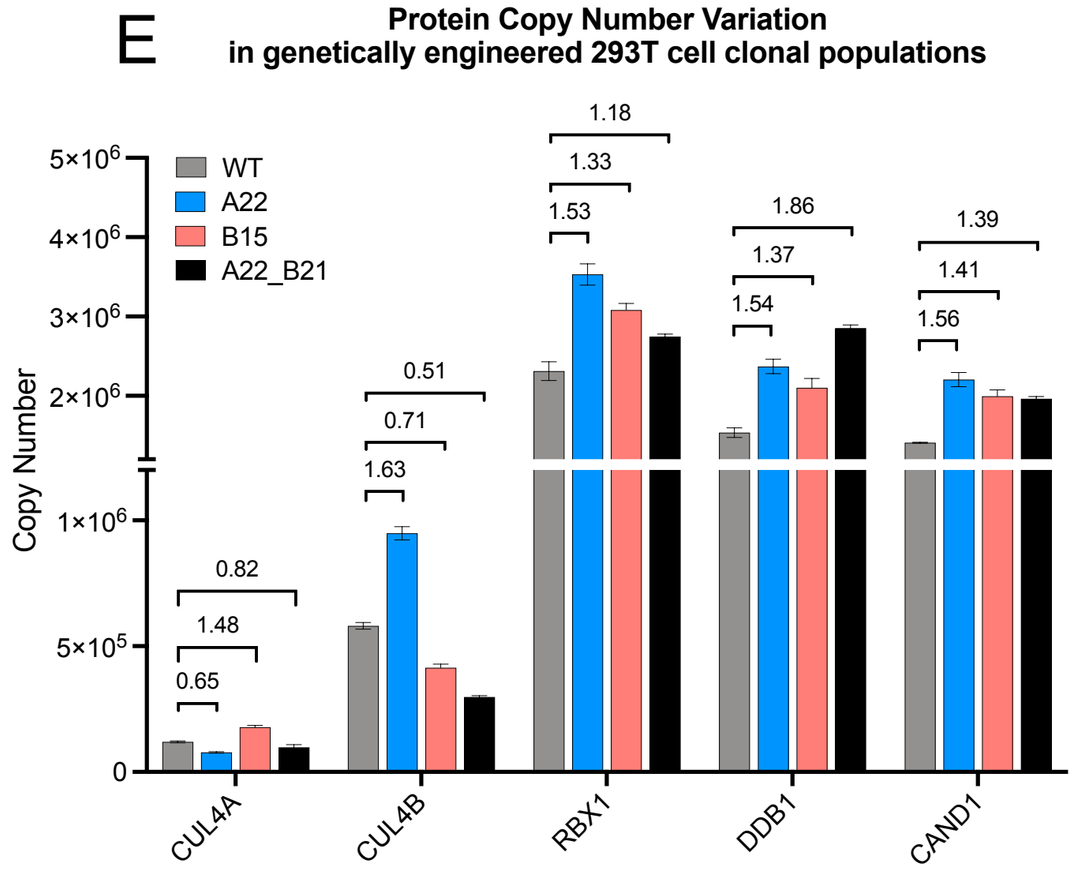

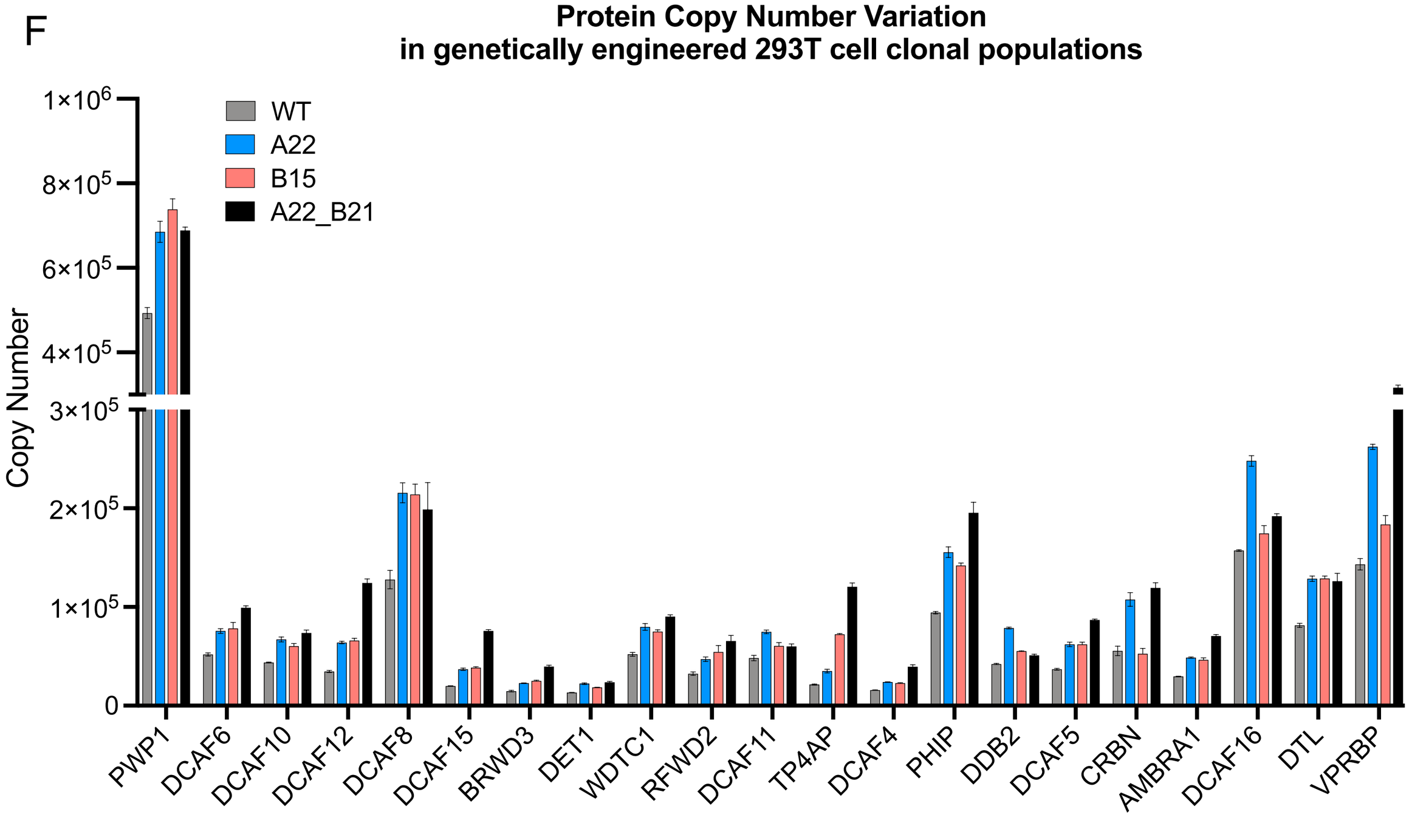

Figure Supplement 8. Assessment of morphology, growth and protein level variation of epitope-tagged cell lines, Related to Figure 1. (A) Light microscopy images of different epitope-tagged cell lines. (B) Assessment of cell growth of parental 293T/17 cells (wild type, WT), 293T/17$^{3xFLAG\text{-}Cul4A}$ (clone A22), 293T/17$^{3xHA\text{-}Cul4B}$ (clone B15), 293T/17$^{3xFLAG\text{-}Cul4A\ \&\ 3xHA\text{-}Cul4B}$ (clone A22_B21) by tracking cell confluency over time via an IncuCyte instrument. (C) The raw data shown in the (B) was used to compute cell doubling time via the formula dT = ln(2) / growth rate. The growth rate (gr) was determined via gr = ln (N(t)/N(0)) / t, where N(1) = confluency at time t, N(0) = confluency at time 0h, and t is the time elapsed between the two measurements. (D) Comparison of total cellular protein content of epitope-tagged cell lines. (E & F) Fresh lysates were prepared from the parental 293T/17 population as well as the clones A22, B15 and A22_B21. CRL4 QconCAT PRM analysis was performed to derive cellular protein copy numbers for each cell line.